# A Pan-Arctic Pigment Database for Phytoplankton and Sea-Ice Algae

## Authors

Asta C. Heidemann[1], Alexander Hayward[2], Philipp Assmy[3], Atreya Basu[4], Astrid Bracher[5,6], Giulia Castellani[6], Giacomo Ditullio[7], Katarzyna Dragańska-Deja[8], Amane Fujiwara[9], Glaucia Moreira Fragoso[10], Jacob Høyer[2], Jiwoon Hwang[11], Morten Iversen[5], Anabel von Jackowski[12], Thomas Juul-Pedersen[13], Piotr Kowalczuk[8], Youngju Lee[14], Maria A. van Leeuwe[15], Atsushi Matsuoka[16], Alenya Merz[13, 17], C. J. Mundy[18], Else Ostermann[13], Ilka Peeken[5], Matt Pinkerton[19], Joanna Stoń-Egiert[8], Jacqueline Stefels[15], Antonia U. Thielecke[5], Gaëlle Veyssiere[20], Hongyan Xi[5], Eun Jin Yang[14] & Rafael Gonçalves-Araujo[1]

## Institution

[1]National Institute of Aquatic Resources, Technical University of Denmark (DTU Aqua), Kgs. Lyngby, Denmark

[2]Danish Meteorological Institute

[3]Norwegian Polar Institute, Fram Centre, Tromsø, Norway

[4]Centre for Earth Observation Science, University of Manitoba, Winnipeg, Canada

[5]Alfred-Wegener-Institute Helmholtz Center for Polar and Marine Research (AWI), Bremerhaven, Germany

[6]Institute of Environmental Physics (IUP), University Bremen (UB), Bremen, Germany

[7]University of Charleston, Grice Marine Laboratory

[8]Institute of Oceanology Polish Academy of Sciences, Sopot, Poland

[9]Institute of Arctic Climate and Environment Research, Japan Agency for Marine-Earth Science and Technology, Yokosuka, Japan

[10]SINTEF Ocean, Department of Climate and Environment, Trondheim, Norway, 7041

[11]University of California, Berkeley, USA

[12]Stockholm University, Stockholm, Sweden

[13]Greenland Climate Research Centre (GCRC), Greenland Institute of Natural Resources (GINR), Nuuk, Greenland

[14]Korea Polar Research Institute, Incheon, Republic of Korea

[15]University of Groningen, Groningen, the Netherlands

[16]Institute for the Study of Earth, Oceans, and Space, University of New Hampshire, USA

[17]Groningen Institute for Evolutionary Life Sciences, University of Groningen, Groningen, Netherlands

[18]Centre for Earth Observation Science, Faculty of Environment, Earth and Resources, University of Manitoba, Winnipeg, Manitoba, Canada

[19]Earth Sciences New Zealand, Wellington, New Zealand

[20]British Antarctic Survey, Cambridge, Cambridgeshire, UK

Correspondence to: Asta C. Heidemann (aheidem@aqua.dtu.dk), Alexander Hayward (algh@dmi.dk) and Rafael Gonçalves-Araujo (rafgo@aqua.dtu.dk)

## Abstract

Climate change has dramatically altered the Arctic seas with significant decrease in sea ice extent and thickness and warming water temperature. The ecological impacts of such change have been described for many parts of the Arctic Ocean, but long-term records of biological indicators are still missing. Among those, photosynthetic and accessory pigments are one of the key tools that aid quantification of phytoplankton and sea-ice algae biomass and characterisation of community composition. To address this gap, we present the first pan-Arctic compilation of in situ algal pigment data obtained exclusively by High-Performance Liquid Chromatography (HPLC), containing 10,798 samples collected across 77 Arctic research cruises between 2000 and 2024. As a result of large-scale collaborative effort, this database covers both open water and sea-ice environments across coastal, shelf and open domains. The database (https://doi.org/10.11583/DTU.29445104) includes measures of up to 26 pigments, with 8 major marker/accessory pigments being considered in this study, namely Alloxanthin (Allo), 19'-Butanoyloxyfucoxanthin (But-fuco), Chlorophyll a (Chl-*a*), Chlorophyll b (Chl-*b*), Fucoxanthin (Fuco), 19'-Hexanoyloxyfucoxanthin (Hex-fuco), Peridinin (Peri), and Zeaxanthin (Zea). This publicly available database provides crucial data that can be used to assess phytoplankton dynamics, validating remote sensing observations and can serve as a resource for future Arctic ecological- and modelling studies.

# 1. Introduction

Climate change has disproportionately affected the Arctic, shown by drastic increases in temperature and ongoing sea-ice decline (England et al., 2021; Stroeve and Notz, 2018). Changing conditions in the Arctic have already altered the food web, with studies indicating further impacts in the near future (Ardyna and Arrigo, 2020; Arrigo and van Dijken, 2015; Flores et al., 2023; Freer et al., 2022; Quinlan et al., 2005). As the foundation of marine food webs, phytoplankton and sea-ice algae are critical for sustaining ecosystems and contribute to large parts of global primary production, leading to energy transfer across trophic levels and ultimately carbon sequestration (Falkowski, 1994; Serra-Pompei et al., 2022). Environmental heterogeneity and changes may alter community composition, with the potential to impact large-scale ecological processes. For example, in the Arctic and sub-Arctic regions, increased open water areas has led to a longer phytoplankton growing season likely associated with changes in community composition. Studies have demonstrated that climate change may favor increased biomass of smaller flagellated phytoplankton species, leading to reduced dominance of large diatoms species (Blais et al., 2017; Coupel et al., 2012; Vonnahme et al., 2025). This can impact the structure of the food web and overall carbon cycling by having an immediate effect on higher trophic levels, potentially influencing the abundance, distribution and feeding preferences of zooplankton (Campbell et al., 2009; Negrete-García et al., 2024).

Characterising phytoplankton community composition is therefore essential for better understanding ecosystem structure, dynamics and services, especially in the under-sampled Arctic seas, which have experienced the greatest impact of climate change in recent years (England et al., 2021). It is clear that long-term data on microalgae physiology and biomass are vital to enhance our ability to assess and detect spatial and temporal patterns in phytoplankton and sea-ice algae community structure and physiology in response to environmental change. Many studies have used pigment-based measurements, but datasets are often scattered across many sources. This makes it difficult to obtain, access and synthesize into a larger spatial and temporal scale. To address this gap, our paper provides baseline information regarding phytoplankton and sea-ice algae biomass and photosynthetic pigments in the Arctic Ocean aiming at providing a framework to support such large-scale Arctic algae studies across two decades of data.

Phytoplankton pigments, particularly chlorophyll a (Chl-*a*), drives photosynthesis by harvesting light and protecting the cells (Falkowski and Kiefer, 1985; Pereira and Gonçalves, 2022). Advances in pigments analysis through High-Performance Liquid Chromatography (HPLC) and ultra HPLC (UHPLC), have enabled precise identification and quantification of a suite of photosynthetic and photoprotective microalgal pigments. These pigments can serve as chemotaxonomic markers for major functional

and taxonomic phytoplankton groups, including the commonly used diagnostic pigments, Alloxanthin (Allo), 19'-Butanoyloxyfucoxanthin (But-fuco), Chlorophyll *b* (Chl-*b*), Fucoxanthin (Fuco), 19'-Hexanoyloxyfucoxanthin (Hex-fuco), Peridinin (Peri), and Zeaxanthin (Zea) used in this study. Additionally and when available, the database presented in this paper also includes α-/β-carotene (αβ-Car), Bacteriochlorophyll a, Chlorophyllide *a* (Chlide *a*), Chl-*c*1, Chl-c1+*c*2, Chl-*c*3, Diadinoxanthin (Diadino), Diatoxanthin (Diato), Divinyl Chlorophyll a and b (DV-Chl-*a* and DV-Chl-*b*), Lutein (Lut), Neoxanthin (Neo), Pheophorbide *a* (Phide *a*), Pheophytin *a* (Phytin *a*), Prasinoxanthin (Pras) and Violaxanthin (Viola) (Jeffrey et al., 1999) (**Table 1**). These additional accessory pigments, some of which are also commonly used as marker pigments (Coupel et al., 2015; Fragoso et al., 2017), enable phytoplankton to adapt and/or acclimate to various light regime changes that occur in the environment (Brunet et al., 2011). Variability in pigment composition can reflect strategies such as photoprotection, which involves the production of pigments that mitigate damage from excessive light and photo acclimation that refers to the ability of algae to adjust their pigment composition in response to light intensity changes that hereby can optimise photosynthetic efficiency (Bonilla et al., 2009; Gosselin et al., 2017).

Absorption and scattering of light by phytoplankton pigments and other cellular constituents influence the reflectance, which allow their detection by radiometers, making them an invaluable source for remote sensing applications (see overview in Bracher et al., 2017). Multispectral satellite sensors such as SeaWiFS, MODIS, MERIS and OLCI have paved the way and demonstrated the ability to distinguish phytoplankton functional types on large scales (Miller, 2004; Nieke et al., 2015). Recent development have focused on hyperspectral sensors, capable of measuring more narrow absorption and reflectance propertied, that can be missed by multispectral sensors (Hu, 2022). Successful applications include ENVISAT's Scanning Imaging Absorption Spectrometer for Atmospheric Chartography (SCIAMACHY) using the PhytoDOAS method (Bracher et al., 2009; Sadeghi et al., 2012) and the DLR Earth Sensing Imaging Spectrometer Mission (DESIS) using the WebAssembly System Interface (WASI) (Gege, 2004, 2014) by (Bracher et al., 2021). Most recently NASA's Plankton, Aerosol, Clouds, ocean Ecosystem (PACE) mission have been launched (Werdell et al., 2024) and the European Space Agency (ESA) is preparing the CHIME hyperspectral to be launched in the coming decade (Nieke et al., 2023).

Since satellites provide long-term synoptic observations of phytoplankton groups high-quality in situ pigment data is invaluable for product validation and algorithm refinement (Cetinić et al., 2024). Similarly, several studies based on self-organizing maps, spectral composition or machine-learning-based methods applied to satellite data have leveraged phytoplankton pigments to understand taxonomic shifts in phytoplankton communities (El Hourany et al., 2019, 2024; Hayward et al., 2025; Xi et al., 2020).

142 ***Table 1***. *Alphabetically ordered list of the major diagnostic pigments and additional accessory pigments considered*
143 *in this study (including abbreviations, their full name and associated phytoplankton groups)* (Fragoso et al., 2017;
144 Jeffrey et al., 1999). *Notice that Dinoflagellates contains two types, reflecting different major pigments.*

| **Major diagnostic pigments** | | |
|---|---|---|
| *Abbreviation* | *Pigment name* | *Associated phytoplankton groups* |
| Allo | Alloxanthin | Cryptophytes |
| But-fuco | 19'-Butanoyloxyfucoxanthin | Haptophytes, Pelagophytes |
| Chl-*a* | Chlorophyll *a* | All phytoplankton groups |
| Chl-*b* | Chlorophyll *b* | Green algae (chlorophytes and prasinophytes) |
| Fuco | Fucoxanthin | Diatoms, Pelagophytes, Dinoflagellates-2, Haptophytes (certain species of *Phaeocystis*) |
| Hex-fuco | 19'-Hexanoyloxyfucoxanthin | Haptophytes, Dinoflagellates-2 |
| Peri | Peridinin | Dinoflagellates-1 |
| Zea | Zeaxanthin | Cyanobacteria, Green algae |

| **Additional accessory pigments** | |
|---|---|
| *Abbreviation* | *Pigment name* |
| αβ-Car | α-/β-carotene |
| Bacteriochlorophyll *a* | Bacteriochlorophyll *a* |
| Chlide *a* | Chlorophyllide *a* |
| Chl-*c*1 | Chlorophyll c1 |
| Chl-*c*1+*c*2 | Chlorophyll c1+c2 |
| Chl-*c*3 | Chlorophyll c3 |
| Diadino | Diadinoxanthin |
| Diato | Diatoxanthin |
| DV-Chl-*a* | Divinyl Chlorophyll *a* |
| DV-Chl-*b* | Divinyl Chlorophyll *b* |
| Lut | Lutein |
| Neo | Neoxanthin |
| Phide *a* | Pheophorbide *a* |
| Phytin *a* | Pheophytin *a* |
| Pras | Prasinoxanthin |
| Viola | Violaxanthin |

145

146 While satellite data is becoming increasingly important, it remains limited by its ability
147 to capture only the first optical depth under cloud- and ice-free conditions.

148 In situ pigment data from the Arctic have compared to other parts of the world
149 historically been limited due to the region's remoteness, harsh weather conditions and
150 logistical challenges of conducting fieldwork in such remote regions. Advances in HPLC
151 technology, together with standardised protocols (Hooker et al., 2005) and round-robins

intercomparison of methodologies (Canuti, 2023), have contributed to the growing availability of pigment data globally, which also includes data from the Arctic and Sub-arctic regions (Kramer et al., 2022; Losa et al., 2017; Mattei and Scardi, 2021; Swan et al., 2016; Xi et al., 2023). Related efforts to obtain pigment data, such as those using UPLC methods (Hwang, 2025), also represent a valuable contribution, though they cannot be incorporated into the current database for inter-comparability reasons with HPLC-based measurements. Despite advances, spatial and temporal coverage across the Arctic remains uneven, underscoring persistent knowledge gaps, highlighting the need for coordinated, collective efforts to compile and expand existing data in this rapidly changing region.

To address this gap, we present the first pan-Arctic overview of phytoplankton and sea-ice algae pigment distributions, based on a comprehensive database of Arctic and sub-Arctic in situ pigment measurements collected between 2000 and 2024. The database is compiled from 77 cruises conducted across the Arctic Ocean, covering coastal, shelf, open-ocean and sea-ice domains (see **Table 2**). Importantly, this database represents a collective effort involving multiple institutions, research teams and international collaborations. By consolidating data from diverse sources, it provides a baseline for assessing long-term trends in phytoplankton pigments, communities and their ecological responses to environmental change. Additionally, such a database can support a pan-Arctic taxonomic characterisation of phytoplankton communities by employing pigment-based taxonomy techniques (Hayward et al., 2023, 2024; Vidussi et al., 2001; Wright and Jeffrey, 2006).

# Methodology

## 2.1. Database Compilation

Phytoplankton and ice algae pigment data was compiled from 77 research cruises conducted between 2000 and 2024. The datasets were sourced from a combination of publicly available repositories (e.g., PANGAEA), institutional databases (e.g., NASA) and personal correspondence with scientists. Datasets were accompanied by relevant ancillary metadata, including information on sampling time, location and depth. A total of 10,798 pigment datapoints were compiled (**Table 2**). Where possible, cruise reports and original publications were consulted to verify the context and methods of data collection. Part of the data has already been published individually for the respective research cruises and/or projects, however, the compiled database presented in this article (including datasets not yet publicly available) has been stored in a public repository (https://doi.org/10.11583/DTU.29445104).

***Table 2**. Alphabetically ordered summary of Arctic and sub-Arctic cruises (= 77) with key dataset information such as year, sampling region(s) (as defined in section 3.1.), environment, sample count and associated DOI, where possible. Note that few samples were from melt-ponds, here assigned as ice samples.*

| Dataset | Year | Region(s) | Environment(s) | Number of Samples | DOI |
|---|---|---|---|---|---|
| ARA06B | 2015 | North Pacific Ocean, East Siberian Sea, Chukchi Sea, CAO | Water | 112 | https://dx.doi.org/doi:10.22663/KOPRI-KPDC-00002844 |
| ARA07B | 2016 | North Pacific Ocean, East Siberian Sea, Chukchi Sea | Water | 50 | |
| ARA08B | 2017 | North Pacific Ocean, East Siberian Sea, Chukchi Sea | Water | 98 | |
| ARA09B | 2018 | East Siberian Sea, Chukchi Sea | Water | 110 | |
| ARA10B | 2019 | North Pacific Ocean, East Siberian Sea, Chukchi Sea | Water | 70 | |
| ARA10B_Ice | 2018 | East Siberian Sea | Ice | 65 | |
| ARA11B | 2020 | North Pacific Ocean, East Siberian Sea, Chukchi Sea | Water | 85 | |
| AREX2000 | 2000 | Norwegian Sea, Barents Sea, Fram Strait | Water | 77 | https://doi.org/10.48457/IOPAN.2025.523 |
| AREX2001 | 2001 | Norwegian Sea, Barents Sea, Fram Strait | Water | 55 | |
| AREX2002 | 2002 | Norwegian Sea, Fram Strait | Water | 20 | |
| AREX2003 | 2003 | Norwegian Sea, Barents Sea, Fram Strait | Water | 50 | |
| AREX2004 | 2004 | Norwegian Sea, Fram Strait | Water | 27 | |
| AREX2005 | 2005 | Norwegian Sea, Barents Sea, CAO, Fram Strait | Water | 51 | |
| AREX2014 | 2014 | Norwegian Sea, Barents Sea, CAO, Fram Strait | Water | 133 | |
| AREX2019 | 2019 | Barents Sea, CAO, Fram Strait | Water | 113 | |
| AREX2021 | 2021 | Norwegian Sea, Barents Sea, Fram Strait | Water | 59 | |
| AREX2022 | 2022 | Norwegian Sea, Barents Sea, CAO, Fram Strait | Water | 140 | |

| | | | | | |
|---|---|---|---|---|---|
| Academik_Ioffe_2003 | 2003 | Greenland Sea, Labrador Sea, Norwegian Sea | Water | 34 | |
| Arc2002 | 2002 | Beaufort Sea, Chukchi Sea | Water | 53 | |
| Arc2004 | 2004 | Beaufort Sea, Chukchi Sea | Water | 90 | |
| Arctic_Ocean_2024 | 2024 | CAO | Ice, Water | 61 | https://doi.org/10.48457/IOPAN.2025.386 |
| Arex2017 | 2017 | CAO, Fram Strait | Water | 33 | |
| Assmy_ICE2010 | 2010 | CAO | Water | 42 | |
| BODC/NERC_2001 | 2001 | Greenland Sea | Water | 169 | http://doi.pangaea.de/10.1594/PANGAEA.793246 |
| BODC/NERC_2002 | 2002 | | | 419 | |
| BaySys | 2018 | Hudson Bay, Labrador Sea | Ice, Water | 131 | https://canwin-datahub.ad.umanitoba.ca/data/dataset/algal-pigments-icewater |
| Bracher2021_PS126 | 2021 | Norwegian Sea, Fram Strait | Water | 175 | https://doi.pangaea.de/10.1594/PANGAEA.982954 |
| Bracher_2017_PS106 | 2017 | Norwegian Sea, Barents Sea, CAO, Fram Strait | Ice, Water | 40 | https://doi.org/10.1594/PANGAEA.899284 |
| Bracher_2019_PS121 | 2019 | Norwegian Sea, Fram Strait | Water | 298 | https://doi.org/10.1594/PANGAEA.941011 |
| Bracher_2020_MSM93 | 2020 | Norwegian Sea, Greenland Sea, Fram Strait | Water | 219 | |
| Bracher_2022_PS131_ATWAICE | 2022 | Norwegian Sea, Greenland Sea, CAO ,Fram Strait | Water | 241 | https://doi.pangaea.de/10.1594/PANGAEA.983242 |
| Bracher_2023_PS136_HAUSGARTEN | 2023 | Norwegian Sea, Fram Strait | Water | 137 | https://doi.pangaea.de/10.1594/PANGAEA.983243 |
| Bracher_2024_PS143.2 | 2024 | Norwegian Sea, CAO, Fram Strait | Water | 212 | https://doi.pangaea.de/10.1594/PANGAEA.983244 |
| CFL | 2008 | Beaufort Sea, Canadian Archipelago | Water | 75 | |
| DANA_ECOTIP_2021 | 2021 | Baffin Bay, Labrador Sea | Water | 16 | https://doi.org/10.48457/IOPAN.2025.523 |
| DSOS_GINR | 2024 | Baffin Bay, Labrador Sea | Water | 234 | |
| DiTuillio_2018 | 2018 | CAO | Water | 132 | 10.18739/A2028PD2H |
| DFO-Fragoso_2005 | 2005 | Labrador Sea | Water | 25 | https://doi.pangaea.de/10.1594/PANGAEA.871872<br><br>For DFO-Fragoso (2005-2013), also see: https://waves-vagues.dfo-mpo.gc.ca/Library/354345.pdf |
| DFO-Fragoso_2006 | 2006 | Labrador Sea | Water | 12 | |
| DFO-Fragoso_2007 | 2007 | Labrador Sea | Water | 32 | |
| DFO-Fragoso_2008 | 2008 | Labrador Sea | Water | 25 | |
| DFO-Fragoso_2009 | 2009 | Labrador Sea | Water | 26 | |
| DFO-Fragoso_2010 | 2010 | Labrador Sea | Water | 27 | |
| DFO-Fragoso_2011 | 2011 | Labrador Sea | Water | 33 | |
| DFO-Fragoso_2012 | 2012 | Labrador Sea | Water | 30 | |
| DFO-Fragoso_2013 | 2013 | Labrador Sea | Water | 27 | |
| Fragoso_2014 | 2014 | Greenland Sea, Labrador Sea | Water | 16 | |
| GreenEdge_Amundsen | 2016 | Baffin Bay, Labrador Sea | Water | 589 | 10.17882/86417 |
| Icescape_2010 | 2010 | Chukchi Sea | Water | 100 | |

| | | | | | |
|---|---|---|---|---|---|
| Icescape_2011 | 2011 | Beaufort Sea, Chukchi Sea | Water | 455 | https://seabass.gsfc.nasa.gov/experiment/ICESCAPE |
| Liu2015_PS93.2 | 2015 | Norwegian Sea, Fram Strait | Water | 241 | |
| Liu_2016_PS99.1 | 2016 | Norwegian Sea, Fram Strait | Water | 96 | https://doi.pangaea.de/10.1594/PANGAEA.905502 |
| Liu_2016_PS99.2 | 2016 | Fram Strait | Water | 230 | https://doi.pangaea.de/10.1594/PANGAEA.894874 |
| Liu_2017_PS107 | 2017 | Norwegian Sea, Fram Strait | Water | 262 | https://doi.pangaea.de/10.1594/PANGAEA.894860 |
| MERIAN_ECOTIP2022 | 2022 | Greenland Sea, Fram Strait | Water | 40 | https://doi.org/10.48457/IOPAN.2025.523 |
| MOSAiC_Algal | 2019, 2020 | CAO, Fram Strait | Ice, Water | 260 | FYI samples: https://doi.pangaea.de/10.1594/PANGAEA.967448<br><br>SYI samples: https://doi.pangaea.de/10.1594/PANGAEA.967450<br><br>Open water samples: https://doi.org/10.1594/PANGAEA.955763 |
| MOSAiC_SYI | 2019, 2020 | CAO | Ice | 275 | |
| MOSAiC_FYI | 2019, 2020 | CAO, Fram Strait | Ice | 285 | |
| MR17-05 | 2017 | Beaufort Sea, North Pacific Ocean, Chukchi Sea | Ice, Water | 74 | https://www.godac.jamstec.go.jp/darwin_cruise/view/metadata?key=MR17-05C&lang=en |
| Malina | 2009 | Baffin Bay, Labrador Sea, Beaufort Sea, Canadian Archipelago, Laptev Sea, North Pacific Ocean, Chukchi Sea | Water | 677 | |
| Malina_Barge | 2009 | Beaufort Sea | Water | 53 | https://www.seanoe.org/data/00641/75345/ |
| N-ICE2015 | 2015 | CAO | Water | 145 | https://doi.org/10.21334/NPOLAR.2016.3EBB7F64 |
| NunaWP4Mackenzie | 2019 | Beaufort Sea | Water | 140 | https://doi.org/10.1594/PANGAEA.937585 |
| Thielecke_PS138_ArcWatch | 2023 | CAO | Ice, Water | 151 | |
| Peeken, PS74 | 2009 | Norwegian Sea, Greenland Sea, Fram Strait | Water | 130 | |
| Peeken, PS76 | 2010 | Norwegian Sea, Greenland Sea, Fram Strait | Water | 549 | |
| Peeken, PS78 | 2011 | Fram Strait | Water | 264 | |
| Peeken, PS80 | 2012 | Laptev Sea, CAO, Fram Strait | Water | 576 | |
| Peeken, PS85 | 2014 | Fram Strait | Water | 82 | |
| Peeken, PS92 | 2015 | CAO | Water | 106 | |

| | | | | | |
|---|---|---|---|---|---|
| Polarstern2003 | 2003 | Greenland Sea, Norwegian Sea | Water | 26 | https://doi.org/10.48457/IOPAN.2025.523 |
| SeaBASS_2004 | 2004 | Beaufort Sea, Chukchi Sea | Water | 59 | |
| SeaBASS_2008 | 2008 | Greenland Sea | Water | 43 | |
| SeaBASS_2013 | 2013 | Baffin Bay, Labrador Sea, Norwegian Sea, Beaufort Sea, Barents Sea, East Siberian Sea, Canadian Archipelago, Chukchi Sea, Greenland Sea, Kara Sea | Water | 77 | |
| SubIce | 2014 | Chukchi Sea | Water | 155 | |
| Tara_Arctic | 2013 | Baffin Bay, Labrador Sea, Norwegian Sea, East Siberian Sea, Barents Sea, Canadian Archipelago, Greenland Sea, Kara Sea | Water | 229 | |
| Woodfjorden | 2024 | Fram Strait | Water | 50 | https://doi.org/10.48457/IOPAN.2025.504 |

## 2.2. Data Quality Measures

This dataset integrated HPLC pigment measurements from 77 research cruises, each carried out by laboratories using their own established laboratory procedures, including different HPLC set-ups, calibration standards and water filtration volume. Methodological descriptions associated with each dataset can be accessed through the provided DOIs in **Table 2** or by contacting the original data providers. To ensure consistency and comparability across sources, we applied a set of inclusion/exclusion criteria and harmonisation procedures to ensure data consistency and comparability across sources. Only datasets with measurements of seven out of the eight marker pigments described in **Table 1** were included in the database, allowing for reliable inter-sample comparison of pigment composition (criterion 1, see **Figure 1**). Although zeaxanthin is normally included in the analysis of phytoplankton functional types, it was excluded as a formal requirement in this database compilation because one source lacked measurement of this pigment and reliable distinction of green algae from other phytoplankton groups remain possible without zeaxanthin (see available pigments for each cruise in Supplementary **S1**). Zeaxanthin is also a major diagnostic pigment for *Synechococcus*, which is largely absent from the Arctic region due to its thermal dependence on warmer waters (Six et al., 2021). Samples were excluded from the final database if they reported Chlorophyll (Chl-*a*) concentration of zero (criterion 2, see

**Figure 1**), lacked measurements of the required marker pigments and/or were missing essential metadata such as geographic coordinates (criterion 3, see **Figure 1**).

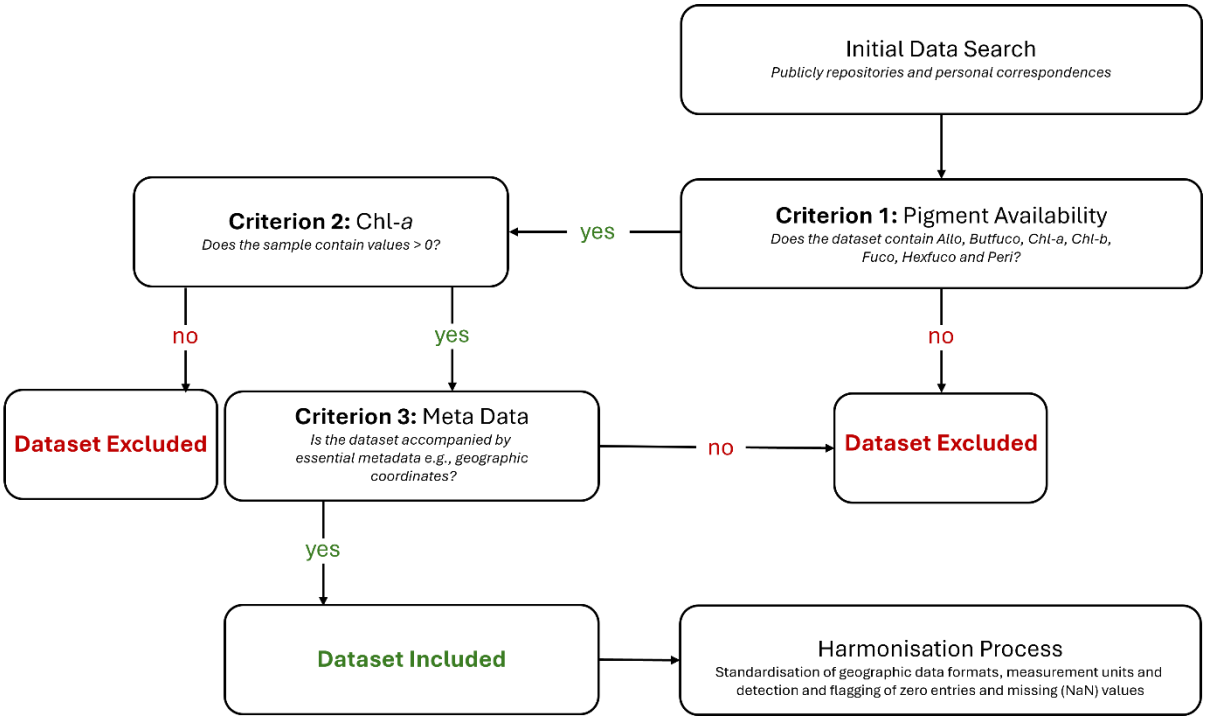


***Figure 1**. Workflow diagram displaying the major decisions in the data compilation process.*

In addition to data filtering, multiple data harmonisation steps were also undertaken: longitudes reported in degrees East (0° to 360°E) were converted to signed longitude (-180° to 180°E/W) to ensure spatial compatibility with standard mapping tools ; datasets were also checked for true 0s and NaNs and that the distinction between these were standardised across datasets. This process required manual inspection of each dataset: If a pigment was entirely absent from a dataset, it was treated as NaNs (empty cells), whereas if a pigment was present but only had a single non-zero value reported, the remaining empty cells were interpreted as true 0s; finally, concentration units for accessory pigments and Chl-*a* were also standardised to the common unit, µg/L. There was considerable variability in methods used to calculate total Chl-*a* was observed across the database, and these methods were not always reported. Consequently, this parameter was excluded. In addition, only a limited number of melt pond samples were available. These were therefore treated as part of the ice sample category, instead of a category by itself.

## 2.3. Limitations and Uncertainties of the Dataset

Despite efforts to minimize both limitations and uncertainties, this dataset consists of HPLC measurements from multiple laboratories. We acknowledge that methodological

variability between laboratories exists and will introduce variability to the dataset. The following sections are provided to summarise the main known sources of limitations and uncertainties associated with compiling HPLC data from various laboratories, as well as general uncertainties inherent to pigments measurements.

### *Analytical*

All datasets presented in this paper have followed standard protocols for HPLC analysis of phytoplankton pigments (see Supplementary Material S2). However, analytical uncertainties can arise from multiple stages of the workflow. As outlined by Wright & Jeffrey (2006), these can broadly be categorised into:

- **Collection and storage**
  Filtration volume, filter type and size, storage temperature and storage time
- **Extraction procedures**
  Sample disruption, duration and temperature, and choice of solvents
- **HPLC methods and techniques** (see review of HPLC pigment methods in Roy et al., 2011)
  Variations of column type and flow rate etc.
- **Peak detection, identification, integration and quantification**
  Differences in baseline correction, peak threshold, co-elution handling and pigment standards used for calibration

To minimize bias in each of these steps, substantial effort has been made through inter-comparability studies. Most notably are the SeaWiFS HPLC Analysis Round-Robin Experiments (SeaHarre-1 to SeaHarre-5) (Hooker et al., 2012) and HPLC/DAD intercomparison on phytoplankton pigments (HIP-1 to HIP-4) (Artuso, F et al., 2016; Canuti et al., 2016), which efforts has been to eliminate differences in pigment quantification across laboratories and quantify these uncertainties in terms of what can be expected, even when conducting analysis according to strict protocols.

### *Pigment-Specific*

In addition to the analytical sources of uncertainties, pigment-specific sources also exist because of a varying degree of sensitivity to the above-described workflow. Any chosen HPLC method can therefore increase or reduce the variance experienced for a specific pigment. However, defining robust “uncertainty values” for each individual pigment remains a challenge across analytical methods. Recent inter-laboratory comparisons highlight this challenge, while also underscoring the need of such estimates in applications such as remote sensing validation (e.g., Canuti, 2023).

A main source of pigment-specific behavior comes from differences in the chemical stability of the pigments. This will affect their susceptibility to degradation, co-elution and extraction efficiency. For example, Chlorophylls (a, b, $c_1$ and $c_2$) are prone to degradation, particularly during storage and extraction, producing degradation products such as pheophytins and chlorophyllides. This can lead to biased and unprecise chlorophyll estimations as well as co-elution issues. This have often been reported for chlorophyll $c_1$ and chlorophyll $c_2$ as well as for the Fuco derivatives (But-fuco and Hex-fuco) (Roy et al., 2011; Simmons et al., 2016; Wright and Jeffrey, 2006; Zapata et al., 2000). Additionally, some chlorophyll degradation products, for example Phide *a* and Phytin *a*, can co-elute with carotenoids due to polarity changes (Mendes et al., 2007).

Finally, pigment concentration itself can be a major source of uncertainty. This is particularly true for low-abundance accessory pigments, which often approach the instrumental limits of detection (LOD) (Bidigare et al., 2002; Canuti, 2023; Canuti et al., 2016; Claustre et al., 2004; Hooker et al., 2005). For instance, when pigment concentrations fall below 0.01 mg $m^{-3}$, the relative standard deviation can reach up to nearly double that of pigments present at higher concentrations (Claustre et al., 2004).

# 3. Data Description

## 3.1. Sampling Coverage

To classify the sampling efforts across the Arctic and sub-Arctic seas into common groups, the study area was subdivided into 15 regions (**Figure 2**). A total of 10,095 water samples and 703 sea-ice samples were compiled and mapped according to their geographic location. Water samples displayed extensive sampling across most regions, while ice samples were comparatively sparse and primarily concentrated in the Central Arctic Ocean (CAO), Canadian Archipelago and Hudson Bay. These samples originate from a limited number of cruises and are not consistently represented throughout the years. Regional sampling frequencies are summarised in **Figure 2**, highlighting the dominance of water samples and the uneven spatial distribution of sea-ice samples.

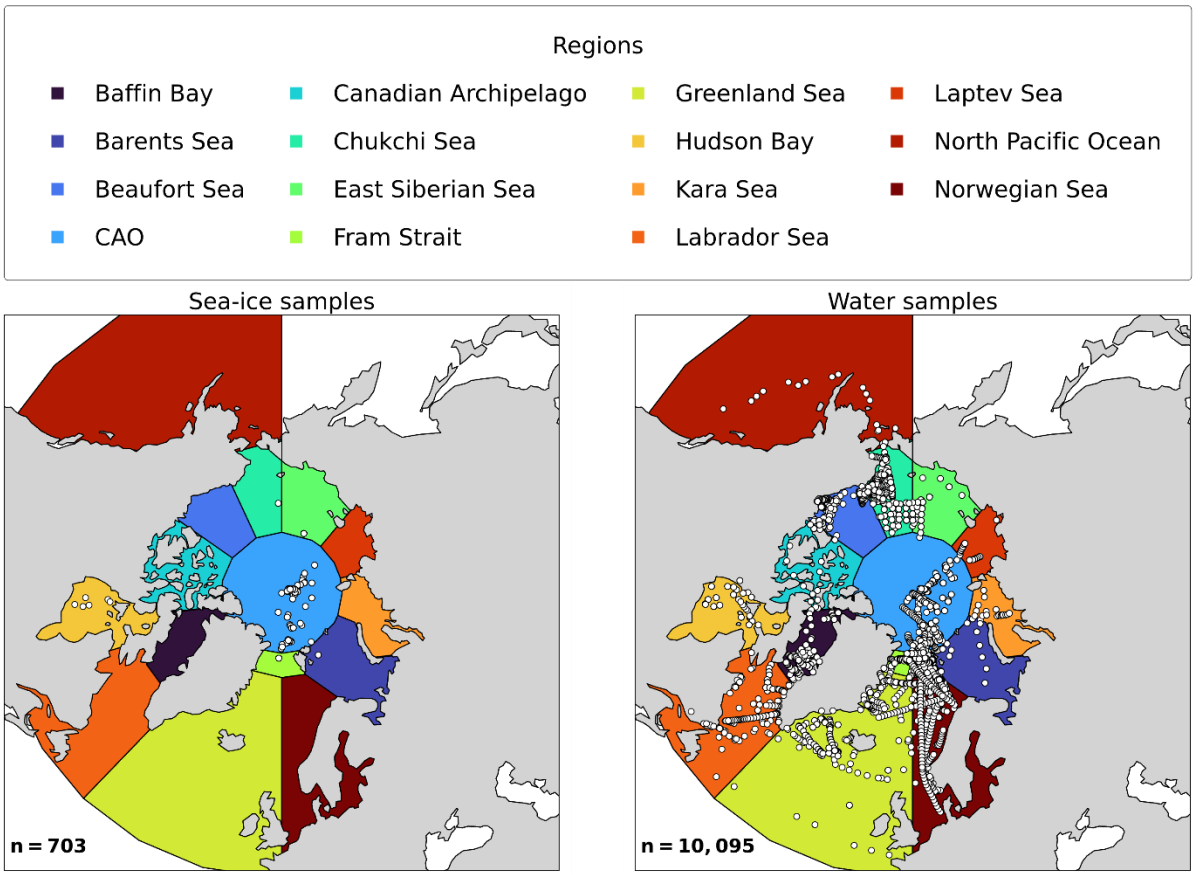


***Figure 2****. Map showing the spatial distribution of water and sea-ice samples across 15 defined regions of the Arctic and sub-Arctic seas. Each point represents an individual sampling location.*

Overall, the water sample collection also varied substantially across years, with higher coverage in 2002, 2009, 2016 and 2020 (**Figure 3**). These periods correspond to large-scale, multidisciplinary campaigns such as MALINA (Coupel et al., 2015), GreenEdge (Bruyant et al., 2022; Massicotte et al., 2020), the AR7W transect during the MOSAiC cruise and others, including global initiatives such as the International Polar Year (IPY). Additionally, the MAREDAT pigment database represents a major synthesis effort (Peloquin et al., 2013) (see **Table 1**).

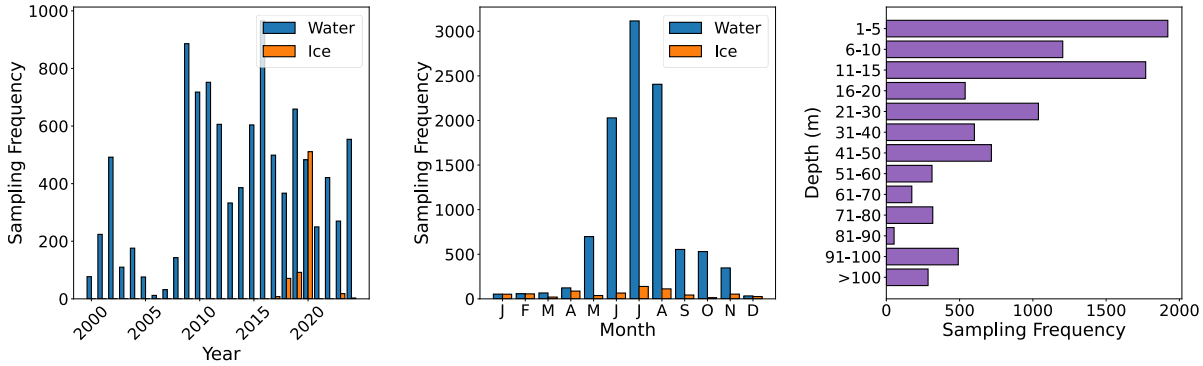


***Figure 3.*** *(Left) yearly sampling frequency for water column and sea-ice samples, (middle) monthly sampling frequency and (right) number of water samples observations per depth bin. Note that for sea-ice samples, the vertical distribution is not presented due to inconsistencies in the ice core sampling methods among the different campaigns.*

Seasonally, sampling frequency was the highest in spring and summer (May-August). Sampling frequency was lower in September, followed by a notable secondary drop in December. The lowest sampling frequency is observed during winter and early spring (December-March), when there is extensive sea ice extent. Sampling frequency also varied vertically in the water column (**Figure 3**). Most samples were collected within the upper 1-15 meters range. Sampling frequency consistently declines from 21-30 meters onward, before a slight increase in the 91-100 meters range.

## 3.2. Pigment Distribution

Pigment concentration in water and sea-ice samples exhibited considerable variability in the biomass and composition of algal communities as well as in the spatiotemporal structure of the database (**Table 3**). In addition, the observed variability can also be attributed to adaptive pigment strategies.

Since direct comparison of absolute pigments concentrations between sea-ice and water samples should be interpreted with caution, only a brief description of absolute pigment concentration is provided for context (**Table 3a**). Chl-*a*, the primary indicator of phytoplankton and sea-ice algae biomass, had a mean concentration of 0.997 µg/L in water samples and 0.639 µg/L in sea-ice samples although the highest individual values in both environments point to episodic blooms. These values represent the mean of all individual concentration measurements in the compiled dataset. The highest concentration across the database, 32.76 µg/L, was recorded in the Chukchi Sea originating from the Ice Scape dataset in August 2010. In general, such high concentrations are rare, with the majority of samples falling below 0.5 µg/L across seasons. Overall, concentrations were highly variable with 90% of values falling between 0.017 and 3.789 µg/L in water samples and between 0.022 and 0.292 µg/L in sea-ice samples (**Table 3a**). It should be recognised that there is a potential bias when comparing open-water and bulk-ice samples due to neglect of the dilution of pigments

when bulk sea-ice cores are melted, which can underestimate concentrations from sympagic algae (Chamberlain et al., 2022; Gradinger, 2009; Miller et al., 2015).

In terms of the relative ratios to Chl-*a* (**Table 3b and Figure 4**) the database also showed marked seasonal variability. Among the eight analysed marker pigments, Fuco consistently had the highest ratios, particularly during winter months, followed by a decline through summer and early autumn. The Fuco-derivatives, But-fuco and Hex-fuco, both considered diagnostic markers of haptophytes, had a stable distribution throughout the year, aside from notable peaks in November.

The ratio of Allo, a distinct marker pigment of cryptophytes, started to increase in late winter, prior to the main growing season. Peri, which is a marker pigment of dinoflagellates, had low overall ratios. These ratios increased during summer, peaking in October, before they exhibited a sharp decline toward the onset of December. As expected, Zea and Chl-*b* were relatively aligned throughout most of the year, consistent with their shared role as a marker pigment of green algae. However, a marked dissimilarity in their patterns occurred in November, when Chl-*b* declined while Zea increased.

For the sea-ice samples, the only accessory pigments with high ratios are Fuco and Chl-*b*.

These differences suggest distinct pigment signatures between sea-ice and water samples, underscoring the importance of expanding sea-ice sampling efforts to better capture algae dynamics in this environment.

***Table 3****. Summary of 5$^{th}$, 95$^{th}$, mean, median and std statistics across all cruises (= 77), for (a) pigment concentration categorized by sample type and (b) relative ratio of accessory pigments vs. Chl-a, For detailed pigment information by individual cruises, see Supplementary* ***Table S1****. For detailed information about all pigments across environments, see Appendices* ***Table A1***

| (a) | **Water Samples (µg/L)** | | | | | **Sea-ice Samples (µg/L)** | | | | |
|---|---|---|---|---|---|---|---|---|---|---|
| Parameter / Pigment | 5$^{th}$ percentile | 95$^{th}$ percentile | Mean | Median | Std | 5$^{th}$ percentile | 95$^{th}$ percentile | Mean | Median | Std |
| Allo | 0.000 | 0.061 | 0.014 | 0.003 | 0.031 | 0.000 | 0.016 | 0.004 | 0.000 | 0.020 |
| But-fuco | 0.000 | 0.080 | 0.020 | 0.007 | 0.040 | 0.000 | 0.005 | 0.001 | 0.000 | 0.008 |
| Chl-*a* | 0.017 | 3.789 | 0.997 | 0.417 | 1.855 | 0.022 | 2.292 | 0.639 | 0.179 | 1.746 |
| Chl-*b* | 0.000 | 0.207 | 0.059 | 0.033 | 0.091 | 0.000 | 0.158 | 0.037 | 0.000 | 0.109 |
| Fuco | 0.003 | 1.493 | 0.357 | 0.106 | 0.853 | 0.000 | 1.392 | 0.367 | 0.063 | 1.120 |
| Hex-fuco | 0.000 | 0.434 | 0.092 | 0.019 | 0.180 | 0.000 | 0.011 | 0.002 | 0.000 | 0.010 |
| Peri | 0.000 | 0.105 | 0.021 | 0.001 | 0.072 | 0.000 | 0.057 | 0.016 | 0.000 | 0.078 |

| Zea | 0.000 | 0.030 | 0.008 | 0.001 | 0.025 | 0.000 | 0.009 | 0.003 | 0.000 | 0.022 |
|---|---|---|---|---|---|---|---|---|---|---|
| (b) | **Water Samples (ratio)** | | | | | **Sea-ice Samples (ratio)** | | | | |
| Parameter / Pigment | 5th percentile | 95th percentile | Mean | Median | Std | 5th percentile | 95th percentile | Mean | Median | Std |
| Allo vs Chl-*a* | 0.000 | 0.078 | 0.100 | 0.009 | 1.634 | 0.000 | 0.034 | 0.006 | 0.000 | 0.021 |
| But-fuco vs Chl-*a* | 0.000 | 0.160 | 0.263 | 0.024 | 4.663 | 0.000 | 0.013 | 0.003 | 0.000 | 0.030 |
| Chl-*b* vs Chl-*a* | 0.000 | 0.358 | 1.094 | 0.077 | 15.482 | 0.000 | 0.414 | 0.087 | 0.000 | 0.138 |
| Fuco vs Chl-*a* | 0.068 | 0.666 | 2.504 | 0.290 | 26.620 | 0.000 | 0.741 | 0.428 | 0.443 | 0.235 |
| Hex-fuco vs Chl-*a* | 0.000 | 0.489 | 0.681 | 0.080 | 9.694 | 0.000 | 0.007 | 0.004 | 0.000 | 0.018 |
| Peri vs Chl-*a* | 0.000 | 0.118 | 0.221 | 0.004 | 5.792 | 0.000 | 0.150 | 0.028 | 0.000 | 0.109 |
| Zea vs Chl-*a* | 0.000 | 0.056 | 0.056 | 0.003 | 1.062 | 0.000 | 0.027 | 0.005 | 0.000 | 0.021 |

370

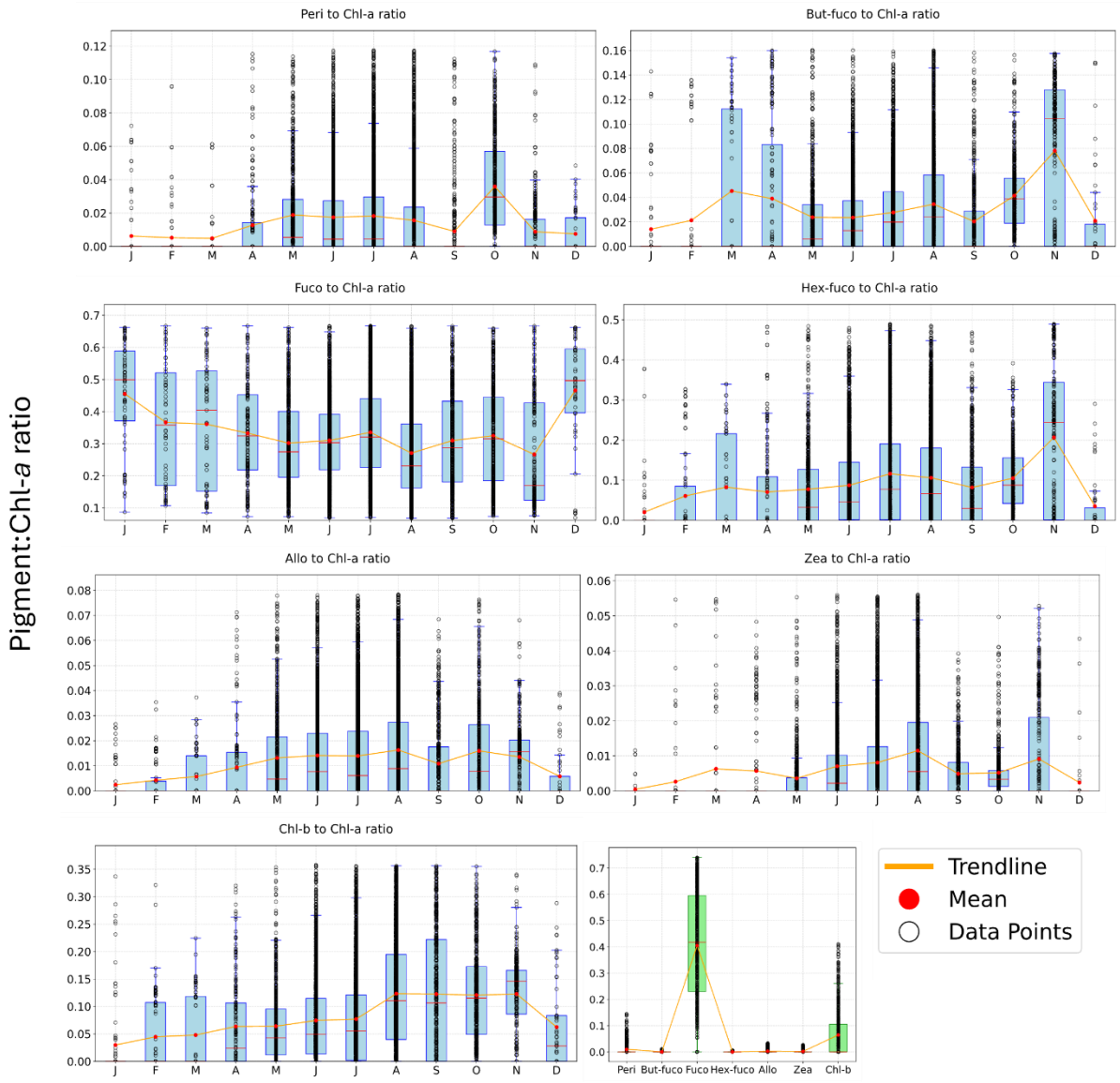


***Figure 4****. Display of the seasonal variation of individual accessory pigment concentration to Chl-a ratio. Water samples are shown as monthly ratios in* ***blue*** *and sea-ice samples are shown overall across months per pigment in* ***green****. Only values within 5$^{th}$ to 95$^{th}$ percentile are included. Data points are displayed as open circles, the mean ratio for each month is shown as a red dot and an orange line connects means.*

## *Spatial and Temporal Dynamics*

In our dataset, Chl-*a* exhibited strong spatial and temporal (seasonal) and inter-annual variability, reflecting the dynamic nature of phytoplankton and sea-ice algae in polar and subpolar environments. Elevated concentrations were observed in areas such as the Fram Strait, Barents Sea, Beaufort Sea, Chukchi Sea and Labrador Sea (**Figure 5**). However, as the database is opportunistic by nature, covering only discrete regional samplings, spatial and seasonal comparisons should be made with caution.

In spring, the Labrador Sea recorded the seasonal maximum (18.75 µg/L), with the highest values occurring mostly in surface waters (0-5 meters). As previously mentioned, summer exhibited the maximum database record for Chl-*a*. Contrary to spring, highest averages were found between 16-30 meters. By autumn, Chl-*a* had declined across most regions. However, localised high biomass persisted in some areas such as Beaufort Sea, Chukchi Sea and Fram Strait. Winter Chl-*a* was generally low.

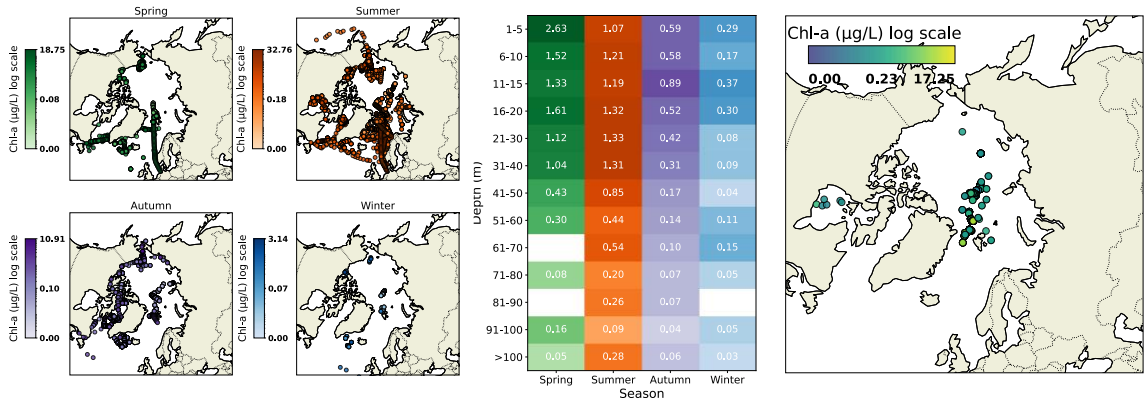


***Figure 5.*** *(a) Spatial distribution of all measured Chl-a water samples in each season, shown as subplots for spring, summer, autumn and winter. Color mapping uses logarithmic scale, but the values themselves are not log-transformed. (b) Mean Chl-a concentration as function of depth range (rows) and season (columns). Color indicates the average value for each depth/season bin. Missing color indicates that data is not available. (c) Spatial distribution of all measured Chl-a for sea-ice samples.*

The concentration frequency distribution plots of water samples (**Figure 6**, blue plots) showed that both Chl-*a*, Chl-*b* and Fuco exhibited approximately log-normal distribution, with peak concentrations near central values and tails on either side. This interpretation was supported by the log-normal distribution of data. However, formal normality tests such as Kolmogorov-Smirnov (K-S test) indicated significant deviations from perfect log-normality, likely due to large sample size and/or the presence of outliers (see Appendices **Figure A1**). In contrast, pigments such as Zea, Peri and the Fuco derivatives exhibited more variable distributions and greater heterogeneity among samples. The histograms for the sea-ice samples (**Figure 6**, grey plots), had much more variability in the distribution of concentrations. This is likely also related to smaller sample size for sea-ice samples.

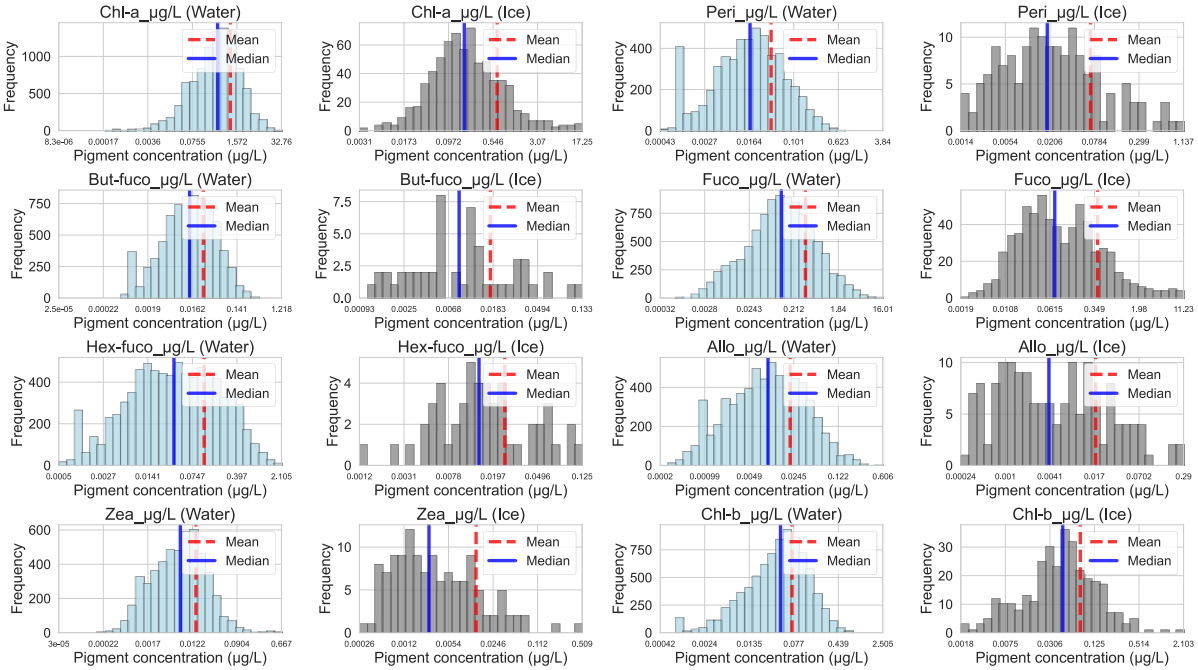


***Figure 6.*** *Frequency histograms displaying log-scaled pigment concentrations. Water samples are shown in blue and sea-ice samples are shown in grey. x-axis represents actual pigment concentrations. Note the different ranges for y-axis comparing water and sea-ice samples.*

## 4. Data Availability

All datasets used in this paper have been compiled into a single repository, accessible using DOI: https://doi.org/10.11583/DTU.29445104 (Heidemann et al., 2026).

## 5. Conclusions

Photosynthetic and accessory pigments serve as indicators of community structure and biomass, and are important oceanographic variables for understanding ocean ecology, as they can also support assessment of biogeochemical cycling. Yet, datasets reporting concentrations of those pigments remain sparse in the Arctic region. To address this gap, we compiled, filtered, standardised and harmonised 10,798 pigment samples from HPLC, including water (n = 10,095) and sea-ice samples (n = 703), collected during 77 research cruises spanning from 2000 to 2024 across 15 defined Arctic and sub-Arctic regions. Sampling frequency varied by year, with peak efforts in 2002, 2009, 2016 and 2020. These years correspond to major multidisciplinary research projects and international initiatives such as the International Polar Year (IPY). Seasonally, most samples were collected during spring and summer months in the upper water column.

Within the available dataset, Chl-*a* was found in higher concentrations in sea-ice samples compared to water samples, on average. However, for accessory pigments, concentrations were generally found to be lower in sea-ice samples. Despite this, the

highest concentration of Chl-*a* across the dataset, 32.76 µg/L, was recorded for a water sample in the Chukchi Sea. Other areas that exhibited elevated Chl-*a* concentrations were spread across the Arctic marginal seas such as the Fram Strait, Barents Sea, Beaufort Sea and Labrador Sea. Interestingly, among the eight marker pigments, Fuco consistently had the highest pigment to Chl-a ratios, particularly during winter months, followed by a decline through summer and early autumn. For the sea-ice samples, the only accessory pigments with high ratios were Fuco and Chl-*b*.

Our comprehensive phytoplankton and sea-ice algal HPLC-based pigment dataset provides valuable insights into the research effort in the Arctic Ocean. Furthermore, it offers important observations on spatial and temporal patterns of primary producers supporting large-scale environmental research in the Arctic across over two decades of sampling efforts.

# Appendices

**Table A1**. *Pigment concentration statistics for all included measured pigments, separated by sample type and summarised across all cruises. For each pigment and environment, the table reports the 5th percentile, 95th percentile, mean, median and standard deviation (Std).*

| | Water Samples (µg/L) | | | | | Sea-ice Samples (µg/L) | | | | |
|---|---|---|---|---|---|---|---|---|---|---|
| Parameter / Pigment | 5th percentile | 95th percentile | Mean | Median | Std | 5th percentile | 95th percentile | Mean | Median | Std |
| Chl *c*3 | 0.000 | 0.232 | 0.054 | 0.014 | 0.116 | 0.000 | 0.051 | 0.014 | 0.000 | 0.053 |
| Chl *c*1*c*2 | 0.000 | 0.652 | 0.146 | 0.048 | 0.295 | 0.000 | 0.365 | 0.101 | 0.035 | 0.254 |
| Chl c1 | 0.000 | 0.031 | 0.009 | 0.000 | 0.061 | 0.000 | 0.000 | 0.000 | 0.000 | 0.007 |
| Chlide *a* | 0.000 | 0.062 | 0.015 | 0.000 | 0.078 | 0.000 | 0.007 | 0.002 | 0.000 | 0.022 |
| Peri | 0.000 | 0.105 | 0.021 | 0.001 | 0.072 | 0.000 | 0.057 | 0.016 | 0.000 | 0.078 |
| Phide *a* | 0.000 | 0.132 | 0.028 | 0.000 | 0.147 | 0.000 | 0.437 | 0.132 | 0.000 | 0.821 |
| But-fuco | 0.000 | 0.080 | 0.020 | 0.007 | 0.040 | 0.000 | 0.005 | 0.001 | 0.000 | 0.008 |
| Fuco | 0.003 | 1.493 | 0.357 | 0.106 | 0.853 | 0.000 | 1.392 | 0.367 | 0.063 | 1.120 |
| Neo | 0.000 | 0.022 | 0.005 | 0.000 | 0.010 | 0.000 | 0.014 | 0.002 | 0.000 | 0.010 |
| Pras | 0.000 | 0.053 | 0.011 | 0.000 | 0.025 | 0.000 | 0.005 | 0.001 | 0.000 | 0.006 |
| Viola | 0.000 | 0.027 | 0.007 | 0.002 | 0.012 | 0.000 | 0.034 | 0.010 | 0.000 | 0.049 |
| Hex-fuco | 0.000 | 0.434 | 0.092 | 0.019 | 0.180 | 0.000 | 0.011 | 0.002 | 0.000 | 0.010 |
| Diadino | 0.000 | 0.232 | 0.058 | 0.020 | 0.108 | 0.000 | 0.239 | 0.052 | 0.000 | 0.208 |
| Allo | 0.000 | 0.061 | 0.014 | 0.003 | 0.031 | 0.000 | 0.016 | 0.004 | 0.000 | 0.020 |
| Diato | 0.000 | 0.025 | 0.005 | 0.000 | 0.016 | 0.000 | 0.063 | 0.010 | 0.000 | 0.036 |
| Zea | 0.000 | 0.030 | 0.008 | 0.001 | 0.025 | 0.000 | 0.009 | 0.003 | 0.000 | 0.022 |
| Lut | 0.000 | 0.011 | 0.003 | 0.000 | 0.012 | 0.000 | 0.025 | 0.009 | 0.000 | 0.069 |
| bacterio chl *a* | 0.000 | 0.000 | 0.000 | 0.000 | 0.001 | 0.000 | 0.000 | 0.000 | 0.000 | 0.000 |
| DV Chl *b* | 0.000 | 0.000 | 0.000 | 0.000 | 0.004 | 0.000 | 0.000 | 0.000 | 0.000 | 0.000 |
| Chl-*b* | 0.000 | 0.207 | 0.059 | 0.033 | 0.091 | 0.000 | 0.158 | 0.037 | 0.000 | 0.109 |
| DV Chl *a* | 0.000 | 0.000 | 0.001 | 0.000 | 0.007 | 0.000 | 0.000 | 0.000 | 0.000 | 0.000 |
| Chl-*a* | 0.017 | 3.789 | 0.997 | 0.417 | 1.855 | 0.022 | 2.292 | 0.639 | 0.179 | 1.746 |
| Phytin *a* | 0.000 | 0.034 | 0.007 | 0.000 | 0.047 | 0.000 | 0.000 | 0.007 | 0.000 | 0.048 |
| alphabetaCar | 0.000 | 0.067 | 0.018 | 0.006 | 0.032 | 0.000 | 0.085 | 0.017 | 0.000 | 0.064 |

**Figure A1**. *Histogram and Q-Q plots performed for each marker pigment on standardised and log-transformed data. For each pigment, a histogram and a Q-Q plot are visualized to assess normality. All Kolmogorov-Smirnov (K-S) p-values were below 0.05 test, indicating that the data deviates from a normal distribution.*

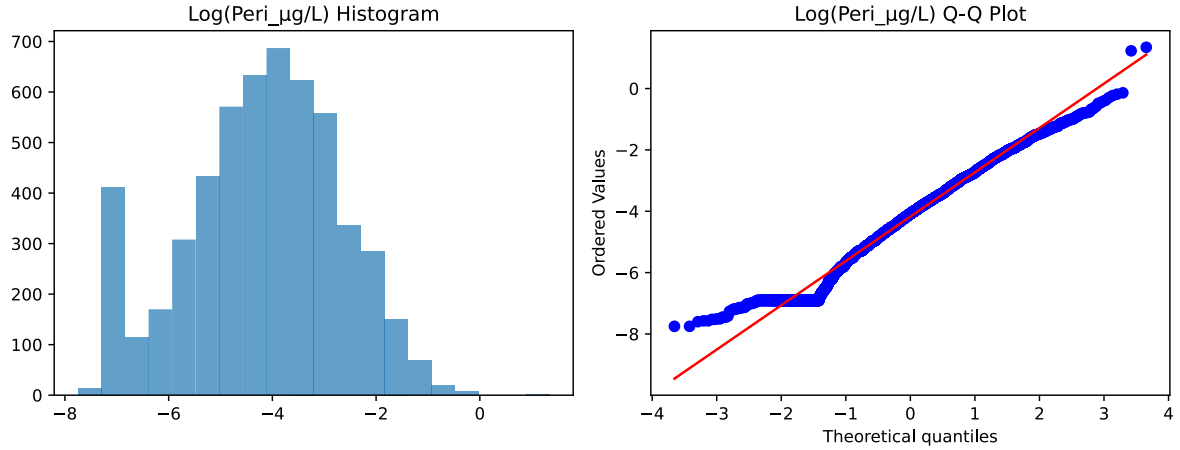


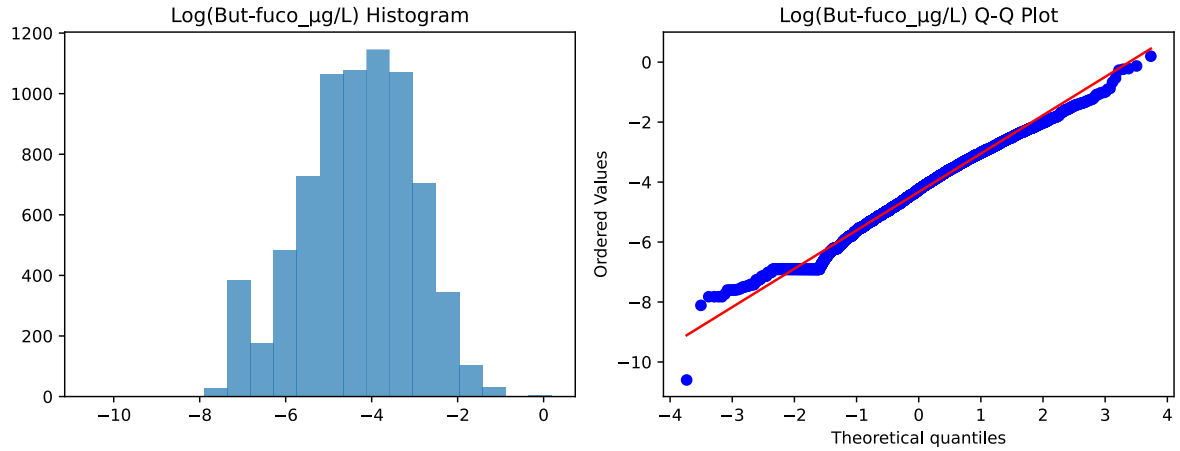


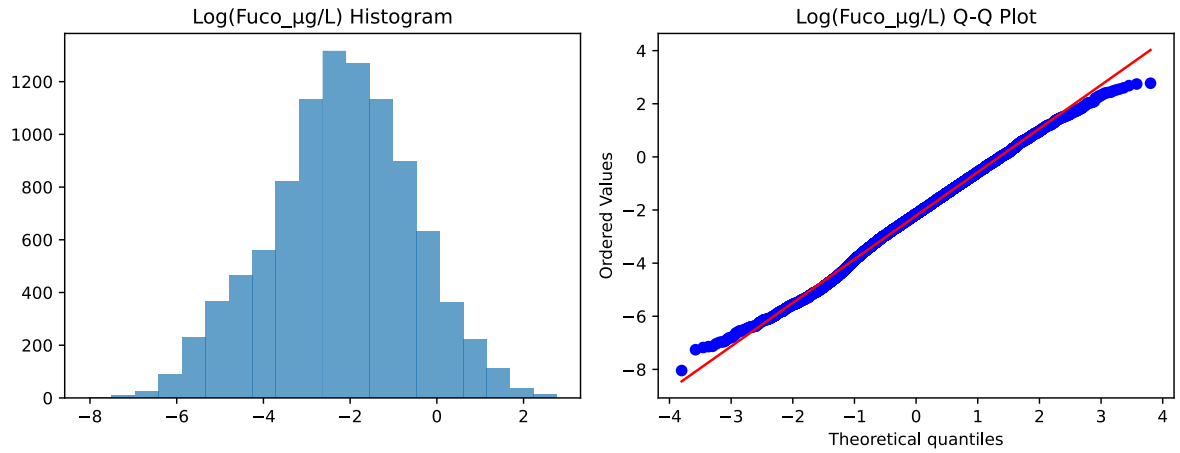

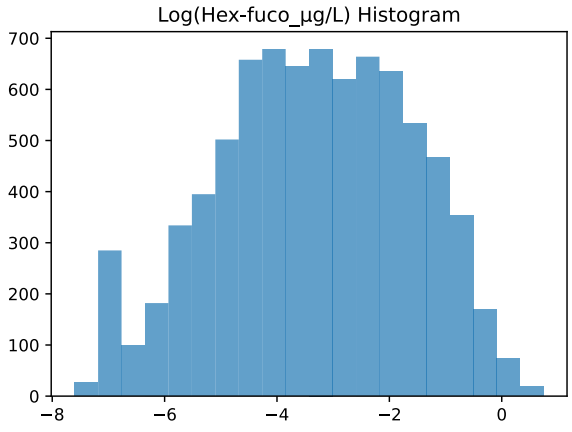
Log(Hex-fuco_µg/L) Histogram
700
600
500
400
300
200
100
0
−8
−6
−4
−2
0

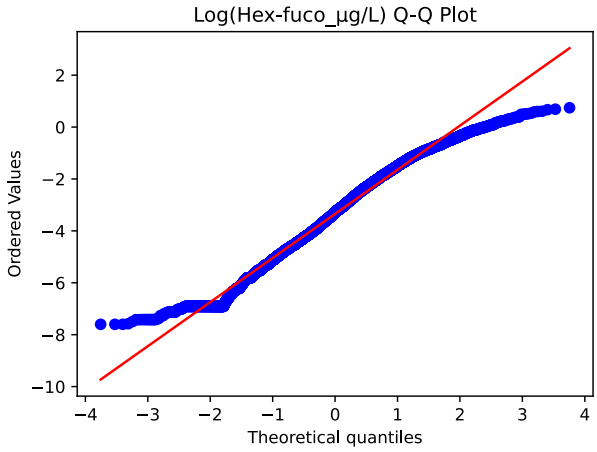
Log(Hex-fuco_µg/L) Q-Q Plot
Ordered Values
2
0
−2
−4
−6
−8
−10
−4
−3
−2
−1
0
1
2
3
4
Theoretical quantiles

461

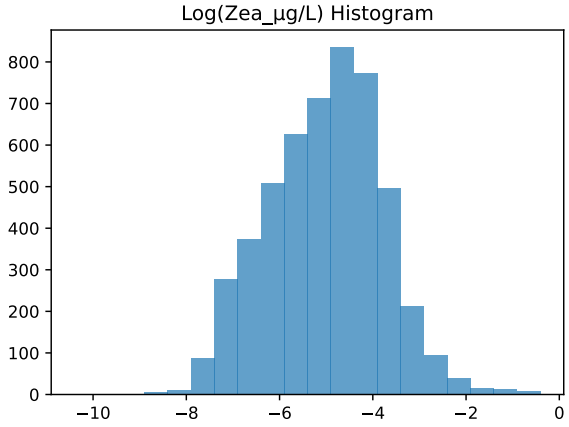
Log(Zea_µg/L) Histogram
800
700
600
500
400
300
200
100
0
−10
−8
−6
−4
−2
0

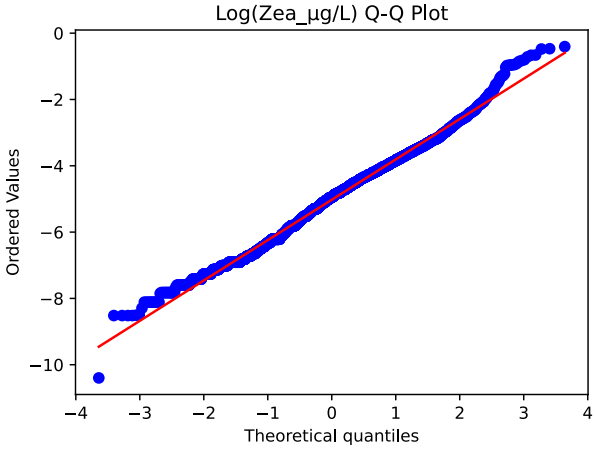
Log(Zea_µg/L) Q-Q Plot
Ordered Values
0
−2
−4
−6
−8
−10
−4
−3
−2
−1
0
1
2
3
4
Theoretical quantiles

462

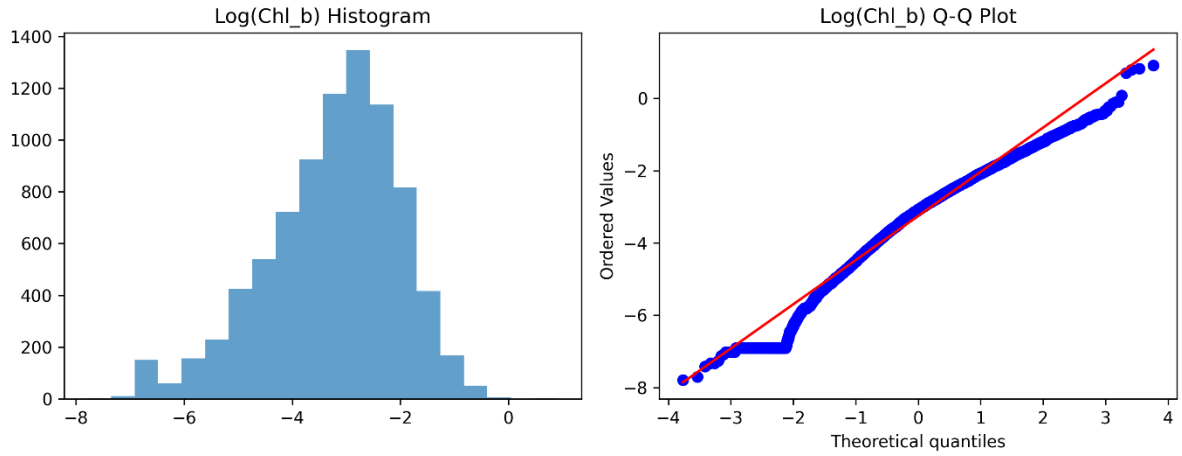


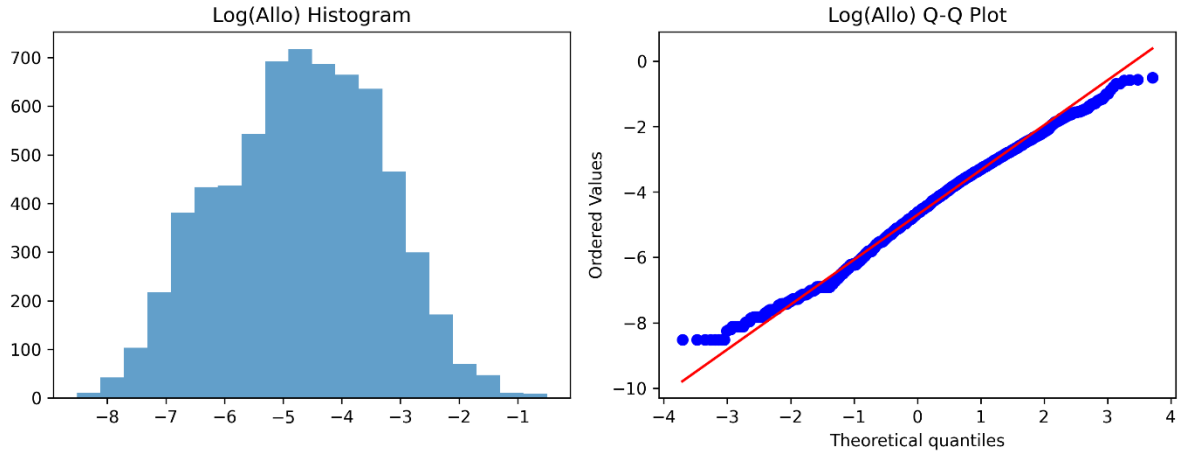


## Author contributions

ACH consolidated the data, harmonized and standardised the dataset, performed the data analysis, generated plots and developed the manuscript.

AH conceived the study idea, provided relevant expertise, contributed data, facilitated key contacts and data sources and contributed to revising and improving the data analysis and manuscript.

RG-A provided relevant expertise and contributed to conceiving the study idea, revising and improving the data analysis and manuscript.

PA, AB (Astrid Bracher), GC, GD, KDD, AF, GMF, JH (Jacob Høyer), MI, AJ, TJP, PK, YL, MAVL, AM (Atsushi Matsuoka), AM (Alenya Merz), CJM, EO, IP, MP, JSE, JS, AT, GV, HX and EJY contributed data, provided relevant expertise and revised the manuscript.

AB (Atreya Basu) and JH (Jiwoon Hwang) provided relevant expertise and revised the manuscript.

## Acknowledgement

ACH and RG-A were supported by the Independent Research Fund Denmark, through the project WaterColor (Gran No. 4251-00058B). RG-A was also supported by the European Union's Horizon Europe research and innovation program under Grant Agreement No. 101136480 (SEA-Quester).

PA was supported by the Research Council of Norway (project no. 244646) and the Ministry of Foreign Affairs, Norway, through the ID Arctic project.

AM was supported by NASA PACE (grant #: 80NSSC26K0091) and JAXA's GCOM-C/SGLI (25RT000334) projects.

YL was supported by Korea Institute of Marine Science and Technology Promotion (KIMST) grant funded by the Ministry of Oceans and Fisheries (KIMST RS-2021-KS211500, Korea-Arctic Ocean Warming and Response of Ecosystem, KOPRI).

KDD, JSE and PK were supported by a project funded by the Polish National Science Centre (NCN) OPUS26 project OptiCal-Green (2023/51/B/ST10/01344) granted to PK. Additional funding has been provided by the European Union's Horizon Europe research and innovation program under Grant Agreement No. 101136480 (SEA-Quester) and under Grant Agreement No. 101136748 (BioEcoOcean), as well as the statutory research program of the Institute of Oceanology, Polish Academy of Sciences (tasks I.2 and II.5). The ship time on board of r/v Kronprins Haakon was provided by the Norwegian Polar Institute, Tromsø, Norway.

GMF was supported by Fisheries and Oceans Canada (DFO). We acknowledge the Atlantic Zone Offshelf Monitoring Program, the captains and crew of the Canadian Coast Guard vessel CCGS *Hudson*, and DFO staff for their contributions to data collection during the Labrador Sea cruises and laboratory analysis at the Bedford Institute of Oceanography

AB and HX were supported by the Helmholtz Infrastructure Initiative FRAM, German Research Foundation (DFG) "Transregional Collaborative Research Center ArctiC Amplification: Climate Relevant Atmospheric and SurfaCe Processes and Feedback Mechanisms (AC)3" (Project C03), Copernicus Marine – Innovation Service Evolution R&D Project ML-PhyTAO (23138L03D-COP-INNO SCI-9000), and the ESA project Phyto-CCI(4000147645/25/I-LR). We thank the captain, the crew and all scientists of RV Polarstern expeditions PS93-2, PS99-2, PS107, PS121, PS126, PS131, PS136 and PS143-2 for their support in preparation and on board the expeditions.

IP was supported by the PoF III & IV program providing ship time on RV Polarstern [Changing Earth –Sustaining our Future, Topic 6.1 of the Helmholtz Association]

AT was supported by the Helmholtz Young Investigator Group SiDe-Effect (VH-NG-1600) awarded to Prof. Mar Fernández-Méndez. PS138 (ArcWatch I) was supported by the Helmholtz Research Programme “Changing Earth – Sustaining our Future” Topic 6, Subtopics 1, 2 and 3 (Grant No. AWI_PS138_02).

JS and MAVL were supported by the Dutch Research Council (NOW), through the Netherlands Polar Programme (NPP), Project no 866. 18. 002.

## References

Ardyna, M. and Arrigo, K. R.: Phytoplankton dynamics in a changing Arctic Ocean, Nat. Clim. Change, 10, 892–903, https://doi.org/10.1038/s41558-020-0905-y, 2020.

Arrigo, K. R. and van Dijken, G. L.: Continued increases in Arctic Ocean primary production, Synth. Arct. Res. SOAR, 136, 60–70, https://doi.org/10.1016/j.pocean.2015.05.002, 2015.

Artuso, F, Canuti, E, Cataldi, D, Costa Goela, P, Grung, M, Ras, J, and Röttgers, R: HPLC/DAD intercomparison on phytoplankton pigments (HIP-1, HIP-2, HIP-3 and HIP-4), Publications Office of the European Union, 2016.

Bidigare, R. R., Van Heukelem, L., and Trees, C. C.: HPLC phytoplankton pigments: sampling, laboratory methods, and quality assurance procedures, Ocean Opt. Protoc. Satell. Ocean Color Sens. Valid. Revis., 3, 258–268, 2002.

Blais, M., Ardyna, M., Gosselin, M., Dumont, D., Bélanger, S., Tremblay, J.-É., Gratton, Y., Marchese, C., and Poulin, M.: Contrasting interannual changes in phytoplankton productivity and community structure in the coastal Canadian Arctic Ocean, Limnol. Oceanogr., 62, 2480–2497, https://doi.org/10.1002/lno.10581, 2017.

Bonilla, S., Rautio, M., and Vincent, W. F.: Phytoplankton and phytobenthos pigment strategies: implications for algal survival in the changing Arctic, Polar Biol., 32, 1293–1303, https://doi.org/10.1007/s00300-009-0626-1, 2009.

Bracher, A., Vountas, M., Dinter, T., Burrows, J. P., Röttgers, R., and Peeken, I.: Quantitative observation of cyanobacteria and diatoms from space using PhytoDOAS on SCIAMACHY data, Biogeosciences, 6, 751–764, https://doi.org/10.5194/bg-6-751-2009, 2009.

Bracher, A., Bouman, H. A., Brewin, R. J. W., Bricaud, A., Brotas, V., Ciotti, A. M., Clementson, L., Devred, E., Di Cicco, A., Dutkiewicz, S., Hardman-Mountford, N. J., Hickman, A. E., Hieronymi, M., Hirata, T., Losa, S. N., Mouw, C. B., Organelli, E., Raitsos, D. E., Uitz, J., Vogt, M., and Wolanin, A.: Obtaining Phytoplankton Diversity from Ocean Color: A Scientific Roadmap for Future Development, Front. Mar. Sci., Volume 4-2017, https://doi.org/10.3389/fmars.2017.00055, 2017.

Bracher, A., Soppa, M. A., Gege, P., Losa, S. N., Silva, B., Steinmetz, F., and Droscher, I.: Extension of Atmospheric Correction Polymer to Hyperspectral Sensors: Application to HICO and First Results for DESIS Data, https://doi.org/10.1109/IGARSS47720.2021.9553568, 2021.

Brunet, C., Johnsen, G., Lavaud, J., and Roy, S.: Pigments and photoacclimation processes, in: Phytoplankton Pigments: Characterization, Chemotaxonomy and Applications in Oceanography, 2011.

Bruyant, F., Amiraux, R., Amyot, M.-P., Archambault, P., Artigue, L., Barbedo de Freitas, L., Bécu, G., Bélanger, S., Bourgain, P., Bricaud, A., Brouard, E., Brunet, C., Burgers, T., Caleb, D., Chalut, K., Claustre, H., Cornet-Barthaux, V., Coupel, P., Cusa, M., Cusset, F., Dadaglio, L., Davelaar, M., Deslongchamps, G., Dimier, C., Dinasquet, J., Dumont, D., Else, B., Eulaers, I., Ferland, J., Filteau, G., Forget, M.-H., Fort, J., Fortier, L., Galí, M., Gallinari, M., Garbus, S.-E., Garcia, N., Gérikas Ribeiro, C., Gombault, C., Gourvil, P., Goyens, C., Grant, C., Grondin, P.-L., Guillot, P., Hillion, S., Hussherr, R., Joux, F., Joy-Warren, H., Joyal, G., Kieber, D., Lafond, A., Lagunas, J., Lajeunesse, P., Lalande, C., Larivière, J., Le Gall, F., Leblanc, K., Leblanc, M., Legras, J., Lévesque, K., Lewis, K.-M., Leymarie, E., Leynaert, A., Linkowski, T., Lizotte, M., Lopes dos Santos, A., Marec, C., Marie, D., Massé, G., Massicotte, P., Matsuoka, A., Miller, L. A., Mirshak, S., Morata, N., Moriceau, B., Morin, P.-I., Morisset, S., Mosbech, A., Mucci, A., Nadaï, G., Nozais, C., Obernosterer, I., Paire, T., Panagiotopoulos, C., Parenteau, M., Pelletier, N., Picheral, M., Quéguiner, B., Raimbault, P., Ras, J., Rehm, E., Ribot Lacosta, L., Rontani, J.-F., Saint-Béat, B., Sansoulet, J., Sardet, N., Schmechtig, C., Sciandra, A., Sempéré, R., et al.: The Green Edge cruise: investigating the marginal ice zone processes during late spring and early summer to understand the fate of the Arctic phytoplankton bloom, Earth Syst. Sci. Data, 14, 4607–4642, https://doi.org/10.5194/essd-14-4607-2022, 2022.

Campbell, R. G., Sherr, E. B., Ashjian, C. J., Plourde, S., Sherr, B. F., Hill, V., and Stockwell, D. A.: Mesozooplankton prey preference and grazing impact in the western Arctic Ocean, Deep Sea Res. Part II Top. Stud. Oceanogr., 56, 1274–1289, https://doi.org/10.1016/j.dsr2.2008.10.027, 2009.

Canuti, E.: Phytoplankton pigment in situ measurements uncertainty evaluation: an HPLC interlaboratory comparison with a European-scale dataset, Front. Mar. Sci., 10, https://doi.org/10.3389/fmars.2023.1197311, 2023.

Canuti, E., Grung, J., Röttgers, M., Goela, C., and Artuso, P.: HPLC/DAD Intercomparison on Phytoplankton Pigments (HIP-1, HIP-2, HIP-3 and HIP-4), https://doi.org/10.2788/47099, 2016.

Cetinić, I., Rousseaux, C. S., Carroll, I. T., Chase, A. P., Kramer, S. J., Werdell, P. J., Siegel, D. A., Dierssen, H. M., Catlett, D., Neeley, A., Soto Ramos, I. M., Wolny, J. L., Sadoff, N., Urquhart, E., Westberry, T. K., Stramski, D., Pahlevan, N., Seegers, B. N., Sirk, E., Lange, P. K., Vandermeulen, R. A., Graff, J. R., Allen, J. G., Gaube, P., McKinna, L. I. W., McKibben, S. M., Binding, C. E., Calzado, V. S., and Sayers, M.: Phytoplankton composition from sPACE: Requirements, opportunities, and challenges, Remote Sens. Environ., 302, 113964, https://doi.org/10.1016/j.rse.2023.113964, 2024.

Chamberlain, E. J., Balmonte, J. P., Torstensson, A., Fong, A. A., Snoeijs-Leijonmalm, P., and Bowman, J. S.: Impacts of sea ice melting procedures on measurements of microbial community structure, Elem. Sci. Anthr., 10, 00017, https://doi.org/10.1525/elementa.2022.00017, 2022.

Claustre, H., Hooker, S. B., Van Heukelem, L., Berthon, J.-F., Barlow, R., Ras, J., Sessions, H., Targa, C., Thomas, C. S., van der Linde, D., and Marty, J.-C.: An intercomparison of HPLC phytoplankton pigment methods using in situ samples: application to remote sensing and database activities, Mar. Chem., 85, 41–61, https://doi.org/10.1016/j.marchem.2003.09.002, 2004.

Coupel, P., Jin, H. Y., Joo, M., Horner, R., Bouvet, H. A., Sicre, M.-A., Gascard, J.-C., Chen, J. F., Garçon, V., and Ruiz-Pino, D.: Phytoplankton distribution in unusually low sea ice cover over the Pacific Arctic, Biogeosciences, 9, 4835–4850, https://doi.org/10.5194/bg-9-4835-2012, 2012.

Coupel, P., Matsuoka, A., Ruiz-Pino, D., Gosselin, M., Marie, D., Tremblay, J.-É., and Babin, M.: Pigment signatures of phytoplankton communities in the Beaufort Sea, Biogeosciences, 12, 991–1006, https://doi.org/10.5194/bg-12-991-2015, 2015.

El Hourany, R., Abboud-Abi Saab, M., Faour, G., Aumont, O., Crépon, M., and Thiria, S.: Estimation of Secondary Phytoplankton Pigments From Satellite Observations Using Self-Organizing Maps (SOMs), J. Geophys. Res. Oceans, 124, 1357–1378, https://doi.org/https://doi.org/10.1029/2018JC014450, 2019.

El Hourany, R., Pierella Karlusich, J., Zinger, L., Loisel, H., Levy, M., and Bowler, C.: Linking satellites to genes with machine learning to estimate phytoplankton community structure from space, Ocean Sci., 20, 217–239, https://doi.org/10.5194/os-20-217-2024, 2024.

England, M. R., Eisenman, I., Lutsko, N. J., and Wagner, T. J. W.: The Recent Emergence of Arctic Amplification, Geophys. Res. Lett., 48, e2021GL094086, https://doi.org/https://doi.org/10.1029/2021GL094086, 2021.

Falkowski, P. and Kiefer, D. A.: Chlorophyll a fluorescence in phytoplankton: relationship to photosynthesis and biomass, J. Plankton Res., 7, 715–731, https://doi.org/10.1093/plankt/7.5.715, 1985.

Falkowski, P. G.: The role of phytoplankton photosynthesis in global biogeochemical cycles, Photosynth. Res., 39, 235–258, https://doi.org/10.1007/BF00014586, 1994.

Flores, H., Veyssière, G., Castellani, G., Wilkinson, J., Hoppmann, M., Karcher, M., Valcic, L., Cornils, A., Geoffroy, M., Nicolaus, M., Niehoff, B., Priou, P., Schmidt, K., and Stroeve, J.: Sea-ice decline could keep zooplankton deeper for longer, Nat. Clim. Change, 13, 1122–1130, https://doi.org/10.1038/s41558-023-01779-1, 2023.

Fragoso, G. M., Poulton, A. J., Yashayaev, I. M., Head, E. J. H., and Purdie, D. A.: Spring phytoplankton communities of the Labrador Sea (2005–2014): pigment signatures,

631 photophysiology and elemental ratios, Biogeosciences, 14, 1235–1259,
632 https://doi.org/10.5194/bg-14-1235-2017, 2017.

633 Freer, J. J., Daase, M., and Tarling, G. A.: Modelling the biogeographic boundary shift of
634 Calanus finmarchicus reveals drivers of Arctic Atlantification by subarctic zooplankton,
635 Glob. Change Biol., 28, 429–440, https://doi.org/https://doi.org/10.1111/gcb.15937,
636 2022.

637 Gege, P.: The water color simulator WASI: an integrating software tool for analysis and
638 simulation of optical in situ spectra, Comput. Geosci., 30, 523–532,
639 https://doi.org/10.1016/j.cageo.2004.03.005, 2004.

640 Gege, P.: WASI-2D: A software tool for regionally optimized analysis of imaging
641 spectrometer data from deep and shallow waters, Comput. Geosci., 62, 208–215,
642 https://doi.org/10.1016/j.cageo.2013.07.022, 2014.

643 Gosselin, M., Rysgaard, S., Lavaud, J., Else, B., Galindo, V., Mundy, C. J., Ehn, J., and
644 Babin, M.: Pigment composition and photoprotection of Arctic sea ice algae during
645 spring, Mar. Ecol. Prog. Ser., 585, 49–69, 2017.

646 Gradinger, R.: Sea-ice algae: Major contributors to primary production and algal
647 biomass in the Chukchi and Beaufort Seas during May/June 2002, Deep Sea Res. Part II
648 Top. Stud. Oceanogr., 56, 1201–1212, https://doi.org/10.1016/j.dsr2.2008.10.016, 2009.

649 Hayward, A., Pinkerton, M. H., and Gutierrez-Rodriguez, A.: phytoclass: A pigment-
650 based chemotaxonomic method to determine the biomass of phytoplankton classes,
651 Limnol. Oceanogr. Methods, 21, 220–241,
652 https://doi.org/https://doi.org/10.1002/lom3.10541, 2023.

653 Hayward, A., Pinkerton, M. H., Wright, S. W., Gutiérrez-Rodriguez, A., and Law, C. S.:
654 Twenty-six years of phytoplankton pigments reveal a circumpolar Class Divide around
655 the Southern Ocean, Commun. Earth Environ., 5, 92, https://doi.org/10.1038/s43247-
656 024-01261-6, 2024.

657 Hayward, A., Wright, S. W., Carroll, D., Law, C. S., Wongpan, P., Gutiérrez-Rodriguez, A.,
658 and Pinkerton, M. H.: Antarctic phytoplankton communities restructure under shifting
659 sea-ice regimes, Nat. Clim. Change, https://doi.org/10.1038/s41558-025-02379-x,
660 2025.

661 Heidemann, A. C., Hayward, A., Assmy, P., Basu, A., Bracher, A., Castellani, G., Ditullio,
662 G., Dragańska-Deja, K., Fujiwara, A., Fragoso, G. M., Høyer, J., Hwang, J., Iversen, M.,
663 von Jackowski, A., Juul-Pedersen, T., Kowalczuk, P., Lee, Y., Matsuoka, A., Merz, A.,
664 Mundy, C. J., Ostermann, E., Pinkerton, M. H., Peeken, I., Stoń-Egiert, J., Thielecke, A. U.,
665 Veyssiere, G., Xi, H., Yang, E. J., and Gonçalves-Araujo, R.: Consolidated Arctic Pigments
666 (2000 to 2024), https://doi.org/https://doi.org/10.11583/DTU.29445104, 2026.

667 Hooker, S. B., Heukelem, L., Thomas, C. S., Claustre, H., Ras, J., Barlow, R., Sessions,
668 H., Schlüter, L., Perl, J., Trees, C., Stuart, V., Head, E., Clementson, L., Fishwick, J.,
669 Llewellyn, C., and Aiken, J.: The Second SeaWiFS HPLC Analysis Round-robin

Experiment (SeaHARRE-2), National Aeronautics and Space Administration, Goddard Space Flight Center, 124 pp., 2005.

Hooker, S. B., Clementson, L., Thomas, C. S., Schlüter, L., Allerup, M., Ras, J., Claire, N., Cullen, J., Kienast, M., Kozlowski, W., Vernet, M., Chakraborty, S., Lohrenz, S., Tuel, M., Redalje, D., Cartaxana, P., Mendes, C. R., Brotas, V., Matondkar, S. G. P., Parab, S. G., Neeley, A., and Egeland, E. S.: The Fifth SeaWiFS HPLC Analysis Round-Robin Experiment (SeaHARRE-5), 2012.

Hu, C.: Hyperspectral reflectance spectra of floating matters derived from Hyperspectral Imager for the Coastal Ocean (HICO) observations, Earth Syst. Sci. Data, 14, 1183–1192, https://doi.org/10.5194/essd-14-1183-2022, 2022.

Hwang, J.: Preliminarily annotated phytoplankton lipids from Polar Cod Connectivity Cruise 2022, https://doi.org/10.5281/zenodo.15085544, 2025.

Jeffrey, S. W., Wright, S. W., and Zapata, M.: Recent advances in HPLC pigment analysis of phytoplankton, Mar. Freshw. Res., 50, 879–896, 1999.

Kramer, S. J., Siegel, D. A., Maritorena, S., and Catlett, D.: Modeling surface ocean phytoplankton pigments from hyperspectral remote sensing reflectance on global scales, Remote Sens. Environ., 270, 112879, https://doi.org/https://doi.org/10.1016/j.rse.2021.112879, 2022.

Losa, S. N., Soppa, M. A., Dinter, T., Wolanin, A., Brewin, R. J. W., Bricaud, A., Oelker, J., Peeken, I., Gentili, B., Rozanov, V., and Bracher, A.: Synergistic Exploitation of Hyper- and Multi-Spectral Precursor Sentinel Measurements to Determine Phytoplankton Functional Types (SynSenPFT), Front. Mar. Sci., 4, https://doi.org/10.3389/fmars.2017.00203, 2017.

Massicotte, P., Amiraux, R., Amyot, M.-P., Archambault, P., Ardyna, M., Arnaud, L., Artigue, L., Aubry, C., Ayotte, P., Bécu, G., Bélanger, S., Benner, R., Bittig, H. C., Bricaud, A., Brossier, É., Bruyant, F., Chauvaud, L., Christiansen-Stowe, D., Claustre, H., Cornet-Barthaux, V., Coupel, P., Cox, C., Delaforge, A., Dezutter, T., Dimier, C., Domine, F., Dufour, F., Dufresne, C., Dumont, D., Ehn, J., Else, B., Ferland, J., Forget, M.-H., Fortier, L., Galí, M., Galindo, V., Gallinari, M., Garcia, N., Gérikas Ribeiro, C., Gourdal, M., Gourvil, P., Goyens, C., Grondin, P.-L., Guillot, P., Guilmette, C., Houssais, M.-N., Joux, F., Lacour, L., Lacour, T., Lafond, A., Lagunas, J., Lalande, C., Laliberté, J., Lambert-Girard, S., Larivière, J., Lavaud, J., LeBaron, A., Leblanc, K., Le Gall, F., Legras, J., Lemire, M., Levasseur, M., Leymarie, E., Leynaert, A., Lopes dos Santos, A., Lourenço, A., Mah, D., Marec, C., Marie, D., Martin, N., Marty, C., Marty, S., Massé, G., Matsuoka, A., Matthes, L., Moriceau, B., Muller, P.-E., Mundy, C.-J., Neukermans, G., Oziel, L., Panagiotopoulos, C., Pangrazi, J.-J., Picard, G., Picheral, M., Pinczon du Sel, F., Pogorzelec, N., Probert, I., Quéguiner, B., Raimbault, P., Ras, J., Rehm, E., Reimer, E., Rontani, J.-F., Rysgaard, S., Saint-Béat, B., Sampei, M., Sansoulet, J., Schmechtig, C., Schmidt, S., et al.: Green Edge ice camp campaigns: understanding the processes controlling the under-ice Arctic phytoplankton spring bloom, Earth Syst. Sci. Data, 12, 151–176, https://doi.org/10.5194/essd-12-151-2020, 2020.

Mattei, F. and Scardi, M.: Collection and analysis of a global marine phytoplankton primary-production dataset, Earth Syst. Sci. Data, 13, 4967–4985, https://doi.org/10.5194/essd-13-4967-2021, 2021.

Mendes, C. R., Cartaxana, P., and Brotas, V.: HPLC determination of phytoplankton and microphytobenthos pigments: comparing resolution and sensitivity of a C18 and a C8 method, Limnol. Oceanogr. Methods, 5, 363–370, https://doi.org/10.4319/lom.2007.5.363, 2007.

Miller, L. A., Fripiat, F., Else, B. G. T., Bowman, J. S., Brown, K. A., Collins, R. E., Ewert, M., Fransson, A., Gosselin, M., Lannuzel, D., Meiners, K. M., Michel, C., Nishioka, J., Nomura, D., Papadimitriou, S., Russell, L. M., Sørensen, L. L., Thomas, D. N., Tison, J.-L., van Leeuwe, M. A., Vancoppenolle, M., Wolff, E. W., and Zhou, J.: Methods for biogeochemical studies of sea ice: The state of the art, caveats, and recommendations, Elem. Sci. Anthr., 3, 000038, https://doi.org/10.12952/journal.elementa.000038, 2015.

Miller, P.: Multi-spectral front maps for automatic detection of ocean colour features from SeaWiFS, Int. J. Remote Sens., 25, 1437–1442, https://doi.org/10.1080/01431160310001592409, 2004.

Negrete-García, G., Luo, J. Y., Petrik, C. M., Manizza, M., and Barton, A. D.: Changes in Arctic Ocean plankton community structure and trophic dynamics on seasonal to interannual timescales, Biogeosciences, 21, 4951–4973, https://doi.org/10.5194/bg-21-4951-2024, 2024.

Nieke, J., Mavrocordatos, C., Donlon, C., Berruti, B., Garnier, T., Riti, J.-B., and Delclaud, Y.: Ocean and Land Color Imager on Sentinel-3, in: Optical Payloads for Space Missions, John Wiley & Sons, Ltd, 223–245, https://doi.org/10.1002/9781118945179.ch10, 2015.

Nieke, J., Despoisse, L., Gabriele, A., Weber, H., Strese, H., Ghasemi, N., Gascon, F., Alonso, K., Boccia, V., Tsonevska, B., Choukroun, P., Ottavianelli, G., and Celesti, M.: The copernicus hyperspectral imaging mission for the environment (CHIME): an overview of its mission, system and planning status, in: Sensors, Systems, and Next-Generation Satellites XXVII, Sensors, Systems, and Next-Generation Satellites XXVII, 21–40, https://doi.org/10.1117/12.2679977, 2023.

Peloquin, J., Swan, C., Gruber, N., Vogt, M., Claustre, H., Ras, J., Uitz, J., Barlow, R., Behrenfeld, M., Bidigare, R., Dierssen, H., Ditullio, G., Fernandez, E., Gallienne, C., Gibb, S., Goericke, R., Harding, L., Head, E., Holligan, P., Hooker, S., Karl, D., Landry, M., Letelier, R., Llewellyn, C. A., Lomas, M., Lucas, M., Mannino, A., Marty, J.-C., Mitchell, B. G., Muller-Karger, F., Nelson, N., O'Brien, C., Prezelin, B., Repeta, D., Jr. Smith, W. O., Smythe-Wright, D., Stumpf, R., Subramaniam, A., Suzuki, K., Trees, C., Vernet, M., Wasmund, N., and Wright, S.: The MAREDAT global database of high performance liquid chromatography marine pigment measurements, Earth Syst. Sci. Data, 5, 109–123, https://doi.org/10.5194/essd-5-109-2013, 2013.

Pereira, L. and Gonçalves, A. M. M.: Plankton Communities, BoD – Books on Demand, 200 pp., 2022.

751 Quinlan, R., Douglas, M. S. V., and Smol, J. P.: Food web changes in arctic ecosystems
752 related to climate warming, Glob. Change Biol., 11, 1381–1386,
753 https://doi.org/10.1111/j.1365-2486.2005.00981.x, 2005.

754 Roy, S., Llewellyn, C. A., Egeland, E. S., and Johnsen, G.: Phytoplankton Pigments:
755 Characterization, Chemotaxonomy and Applications in Oceanography, Cambridge
756 University Press, 891 pp., 2011.

757 Sadeghi, A., Dinter, T., Vountas, M., Taylor, B. B., Altenburg-Soppa, M., Peeken, I., and
758 Bracher, A.: Improvement to the PhytoDOAS method for identification of
759 coccolithophores using hyper-spectral satellite data, Ocean Sci., 8, 1055–1070,
760 https://doi.org/10.5194/os-8-1055-2012, 2012.

761 Serra-Pompei, C., Ward, B. A., Pinti, J., Visser, A. W., Kiørboe, T., and Andersen, K. H.:
762 Linking Plankton Size Spectra and Community Composition to Carbon Export and Its
763 Efficiency, Glob. Biogeochem. Cycles, 36, e2021GB007275,
764 https://doi.org/https://doi.org/10.1029/2021GB007275, 2022.

765 Simmons, L. J., Sandgren, C. D., and Berges, J. A.: Problems and pitfalls in using HPLC
766 pigment analysis to distinguish Lake Michigan phytoplankton taxa, J. Gt. Lakes Res., 42,
767 397–404, https://doi.org/10.1016/j.jglr.2015.12.006, 2016.

768 Six, C., Ratin, M., Marie, D., and Corre, E.: Marine Synechococcus picocyanobacteria:
769 Light utilization across latitudes, Proc. Natl. Acad. Sci., 118, e2111300118,
770 https://doi.org/10.1073/pnas.2111300118, 2021.

771 Stroeve, J. and Notz, D.: Changing state of Arctic sea ice across all seasons,
772 https://doi.org/10.1088/1748-9326/aade56, 2018.

773 Swan, C. M., Vogt, M., Gruber, N., and Laufkoetter, C.: A global seasonal surface ocean
774 climatology of phytoplankton types based on CHEMTAX analysis of HPLC pigments,
775 Deep Sea Res. Part Oceanogr. Res. Pap., 109, 137–156,
776 https://doi.org/https://doi.org/10.1016/j.dsr.2015.12.002, 2016.

777 Vidussi, F., Claustre, H., Manca, B. B., Luchetta, A., and Marty, J.-C.: Phytoplankton
778 pigment distribution in relation to upper thermocline circulation in the eastern
779 Mediterranean Sea during winter, J. Geophys. Res. Oceans, 106, 19939–19956,
780 https://doi.org/10.1029/1999JC000308, 2001.

781 Vonnahme, T. R., Chitkara, C., Krawczyk, D., Meire, L., Skogseth, R., Vader, A., and Juul-
782 Pedersen, T.: Abrupt decline of microplankton species richness linked to coastal inflow
783 in an Arctic fjord, Limnol. Oceanogr., 70, 2688–2702, https://doi.org/10.1002/lno.70159,
784 2025.

785 Werdell, P. J., Franz, B., Poulin, C., Allen, J., Cairns, B., Caplan, S., Cetinić, I., Craig, S.,
786 Gao, M., Hasekamp, O., Ibrahim, A., Knobelspiesse, K., Mannino, A., Martins, J. V.,
787 McKinna, L., Meister, G., Patt, F., Proctor, C., Rajapakshe, C., Ramos, I. S., Rietjens, J.,
788 Sayer, A., and Sirk, E.: Life after launch: a snapshot of the first six months of NASA's
789 Plankton, Aerosol, Cloud, Ocean Ecosystem (PACE) mission, in: Sensors, Systems, and

790 Next-Generation Satellites XXVIII, Sensors, Systems, and Next-Generation Satellites
791 XXVIII, 70–84, https://doi.org/10.1117/12.3033830, 2024.

792 Wright, S. W. and Jeffrey, S. W.: Pigment Markers for Phytoplankton Production, in:
793 Marine Organic Matter: Biomarkers, Isotopes and DNA, edited by: Volkman, J. K.,
794 Springer Berlin Heidelberg, Berlin, Heidelberg, 71–104,
795 https://doi.org/10.1007/698_2_003, 2006.

796 Xi, H., Losa, S. N., Mangin, A., Soppa, M. A., Garnesson, P., Demaria, J., Liu, Y., d'Andon,
797 O. H. F., and Bracher, A.: Global retrieval of phytoplankton functional types based on
798 empirical orthogonal functions using CMEMS GlobColour merged products and further
799 extension to OLCI data, Remote Sens. Environ., 240, 111704,
800 https://doi.org/10.1016/j.rse.2020.111704, 2020.

801 Xi, H., Peeken, I., Gomes, M., Brotas, V., Tilstone, G. H., Brewin, R. J. W., Dall'Olmo, G.,
802 Tracana, A., Alvarado, L. M. A., Murawski, S., Wiegmann, S., and Bracher, A.:
803 Phytoplankton pigment concentrations and phytoplankton groups measured on water
804 samples collected from various expeditions in the Atlantic Ocean from 71°S to 84°N,
805 https://doi.org/10.1594/PANGAEA.954738, 2023.

806 Zapata, M., Rodríguez, F., and Garrido, J. L.: Separation of chlorophylls and carotenoids
807 from marine phytoplankton: a new HPLC method using a reversed phase C8 column
808 and pyridine-containing mobile phases, Mar. Ecol. Prog. Ser., 195, 29–45,
809 https://doi.org/10.3354/meps195029, 2000.

810

811

812